NACA

RESEARCH MEMORANDUM

INVESTIGATION OF THE AERODYNAMIC CHARACTERISTICS AT HIGH

SUPERSONIC MACH NUMBERS OF A FAMILY OF DELTA WINGS

HAVING DOUBLE-WEDGE SECTIONS WITH THE

MAXIMUM THICKNESS AT 0.18 CHORD

By Mitchel H. Bertram and William D. McCauley

Langley Aeronautical Laboratory
Langley Field, Va.

NATIONAL ADVISORY COMMITTEE
FOR AERONAUTICS

WASHINGTON

October 20, 1954
Declassified July 17, 1958

ERRATA

NACA RM L54G28

INVESTIGATION OF THE AERODYNAMIC CHARACTERISTICS AT HIGH
SUPERSONIC MACH NUMBERS OF A FAMILY OF DELTA WINGS
HAVING DOUBLE-WEDGE SECTIONS WITH THE
MAXIMUM THICKNESS AT 0.18 CHORD
By Mitchel H. Bertram and William D. McCauley

October 20, 1954

Page 11, lines 1 to 20: The discussion in paragraphs 1 and 2 is mis-
  leading, since the theoretical skin-friction coefficients given are
  based on an erroneous value of the effective chord. Lines 1 to 20 on
  this page should therefore be deleted and replaced by the following
  paragraph:

    The laminar skin-friction values used for wings 1, 2, and 3 were
  empirically determined from an examination of the data for the wings
  with attached shocks from this investigation and data from 2.5- and
  5-percent-thick double-wedge-section delta wings tested at $M = 6.9$.
  Good agreement with the data was obtained when $C_f \sqrt{R} = 4.89$ and
  the pressure-drag coefficient was assumed to be equal to that for the
  wing section (in the streamwise direction). On the assumption that
  the flow was partly conical in nature for wings 4 and 5 with detached
  shocks, the empirical coefficient $C_f \sqrt{R} = 4.89$ was modified slightly
  to $C_f \sqrt{R} = 4.66$.

Page 42: The label for the top curve in figure 6 should have the paren-
  thetical statement "(based on triangular flat plate)" deleted.

NATIONAL ADVISORY COMMITTEE FOR AERONAUTICS

RESEARCH MEMORANDUM

INVESTIGATION OF THE AERODYNAMIC CHARACTERISTICS AT HIGH

SUPERSONIC MACH NUMBERS OF A FAMILY OF DELTA WINGS

HAVING DOUBLE-WEDGE SECTIONS WITH THE

MAXIMUM THICKNESS AT 0.18 CHORD

By Mitchel H. Bertram and William D. McCauley

SUMMARY

A program to investigate the aerodynamic characteristics of a family of delta wings with a blunt double-wedge section has been conducted at the Langley 11-inch hypersonic tunnel. These wings had a maximum thickness of 8 percent of the chord located at the 18-percent-chord point. For the wings tested at a Mach number of 6.9, the semiapex angle was varied from 30° to 5° and the wings were tested over a range of angle of attack from 0° to 28° and Reynolds numbers in the range of 0.8×10^6 to 3.6×10^6 based on root chord. In addition, pertinent results from tests at Mach numbers as low as 1.62 have been utilized. The shock-expansion theory and the Newtonian impact theory have been used to analyze the effects of changes made in the various parameters investigated.

The lift and drag coefficients were found to lie in the region bounded by the two-dimensional shock-expansion theory and the Newtonian impact theory.

Consideration of the available data for these wings at Mach numbers between 1.62 and 6.9 indicates that when the leading-edge shock wave is detached the drag and lift-curve slope at zero angle of attack for a given semiapex angle tend toward the values given by two-dimensional shock-expansion theory with increasing Mach number when the semiapex angle is equal to or greater than 22°. For semiapex angles less than 22° the data indicate that the trend with increasing Mach number is to approach the approximate value for the particular wing given by the impact theory.

The lift-drag ratio increases with decreases in semiapex angle due mainly to a rapid decrease in chord force as the angle of attack increases.

INTRODUCTION

There are relatively little data for lifting wings in the Mach number range above about 3. At Mach number 6.9 there are the data obtained by McLellan, Bertram, and Moore (ref. 1), and McLellan (ref. 2), and at Mach number 4.04 there is the information variously obtained by Ulmann, Lord, Dunning, and Smith (refs. 3 to 6). Reference 7 presents much of the available data for thin delta wings in the range of Mach numbers from 1.6 to 6.9. Much of the data in references 1 to 7 are for plan forms other than delta.

Force predictions for thin delta wings can be obtained through application of the linear theory developed by Puckett, Robinson, Stewart, and Brown (refs. 8 to 12) which allows separate consideration for the effects of thickness (on the drag), camber, and angle of attack. However, the accuracy of these predictions of the aerodynamic forces depends upon whether the shock is attached since even at the lower supersonic Mach numbers force predictions for wings where the shock is detached can be rather poor and, in addition, at the higher Mach numbers the lift becomes significantly dependent upon the wing section, whereas the lift derived from linear theory is based on a wing with zero thickness. A recent investigation by Ulmann and Bertram (ref. 7) shows that two-dimensional shock-expansion theory in combination with linear theory may be applied to thin delta wings to obtain accurate predictions of lift-curve slope and minimum drag if a modification of the theory is assumed to account for shock detachment.

Wings whose thickness distribution no longer allow the designation "thin" are of interest and for such wings the linear theory or its modifications would not be expected to give accurate predictions for the aerodynamic characteristics. In this case, other theoretical methods such as shock-expansion theory and Newtonian impact theory must be used. Wings with a relatively thick section have been tested by Love (ref. 13) at Mach numbers from 1.62 to 2.40. These wings were 8 percent thick at the 18-percent-chord point. In order to extend the Mach number range of these data, the present investigation was planned to test wings with a delta plan form at Mach number 6.9 with the same thickness distribution as those tested by Love. The semiapex angle was varied from 30° to 5° and the wings were tested over a range of angle of attack from 0° to 28° and Reynolds numbers based on root chord in the range of 0.8×10^6 to 3.6×10^6.

SYMBOLS

S	plan-form area
c	chord length
C_C	chord-force coefficient, $\dfrac{\text{Chord force}}{qS}$
C_L	lift coefficient, $\dfrac{\text{Lift}}{qS}$
C_D	drag coefficient, $\dfrac{\text{Drag}}{qS}$
$C_{M2/3}$	moment coefficient about the 2/3 root chord point, $\dfrac{M_{2/3}}{qSc_r}$
C_N	normal-force coefficient
C_f	average skin-friction coefficient
C.P.	center of pressure measured from wing-apex in fractions of root chord
D	drag
L	lift
M	Mach number
$M_{2/3}$	moment about 2/3 root chord point
m	Mach angle corresponding to free-stream Mach number
R	Reynolds numbers based on root chord
t	thickness
α	angle of attack of wing
ϵ	semiapex angle of wing
γ	ratio of the specific heat at constant pressure to that at constant volume

Subscripts:

∞ two dimensional

0 zero angle of attack

i inviscid

r root

APPARATUS AND METHODS

Tunnel

This investigation was conducted in the Langley 11-inch hypersonic tunnel, an intermittent blowdown tunnel, which for these tests utilized a single-step two-dimensional nozzle with a central core of uniform flow approximately 5 inches square. The Mach number in this central core is approximately 6.90. A description of the tunnel may be found in reference 14 and a description of the nozzle and its calibration at a stagnation pressure of 25 atmospheres in reference 15.

Instrumentation

The measurement of the forces on the models was accomplished through the use of two, two-component strain-gage balances of different sensitivities and a balance for the measurement of pitching moment. The more sensitive two-component balance was used in the low angle-of-attack range and measured forces normal and parallel to the wing chord. The other two-component balance measured lift and drag directly and was used for moderate and high angles of attack. The balances are temperature compensated and the sensitivity to uneven heating effects has been reduced to tolerable limits by insulation. For a more detailed description of the two-component balances, see reference 1.

The base and balance pressures for use with the sting corrections were measured by means of an aneroid type six-cell recording unit described in reference 14. The stagnation pressure was measured with Bourdon tube gages with an accuracy of 1/2 to 1 percent.

Models and Supports

The five wings investigated had double-wedge sections in the free-stream direction and were symmetrical about the chord with the maximum

thickness of 8 percent of the chord located at the 18-percent-chord point.
The largest wing semiapex angle was 30° and the smallest semiapex angle
was 5°. These wings are shown in table 1 and a photograph of wings 2
and 5 on their mounting sting is presented in figure 1(a). The surfaces
were ground and the leading edges were from 0.001 to 0.002 inch thick.
The wings were supported on stings whose pertinent dimensions are shown
in figure 1(b).

Schlieren System

A schlieren system was used to study flow characteristics and obtain
the angle of attack. At present, a horizontal single-pass system is
employed. The system incorporates a horizontal knife edge, and film
exposures are of several microseconds duration. The angle of attack was
measured from the schlieren film negatives to within 0.2° through the use
of an optical comparator.

Surface Film Flow Studies

Surface flow studies of wings 2 and 5 were made by photographing the
patterns made by streaming graphite and fluorescing mineral oil under
ultraviolet light during a run. The wings were coated with SAE-30 lubri-
cating oil before the run and graphite was spotted along the leading edge.
Views of wing 2 were obtained both with a 35-millimeter still camera and
with a 16-millimeter motion-picture camera, whereas wing 5 was photo-
graphed only with the motion-picture camera. The cameras were equipped
with suitable filters to photograph the fluorescing oil to best advantage.

TUNNEL CONDITIONS

During the tests the tunnel was operated at a stagnation temperature
of about 1130° R and through a stagnation pressure range from 15
to 40 atmospheres. An exception to these conditions was the surface film
flow tests where the temperature was purposely maintained somewhat lower,
averaging about 1090° R. The air was heated by being passed through an
electrical heater with Nichrome tube resistance elements which replaces
the storage heater of references 1, 2, 14, and 15. The model Reynolds
numbers (based on root chord) varied from about 0.8×10^6 to 3.6×10^6.
The length of the test runs varied from 60 to 75 seconds. The data were
evaluated at 55 seconds after the start of each run in order to reduce
the effects of a slight Mach number variation with time during the run.
Recent nozzle calibration shows that at this time during the run the Mach
number is 6.90 at a stagnation pressure of 33 atmospheres. At a stagna-
tion pressure of 21 atmospheres, calibrations have indicated a Mach number

of 6.84 at this time while Mach numbers of 6.86 and 6.92 are indicated
at stagnation pressures of 25 and 37 atmospheres, respectively.

Errors in coefficients can arise from errors in evaluating the Mach
number, stagnation pressure, and angle of attack as well as inherent
errors introduced by aerodynamic heating effects on the balance and inter-
action of the force components. The maximum error possible at several
values of C_L and C_D due to these factors is believed to be as shown
in the following table for the pressure at which most of the lifting wing
data were obtained.

Balance	C_L	Percent error	C_D	Percent error
1 (sensitive)	0.01 .02 .13	10 7 5	0.016 .043	3.5 5
2	.22 .45	4 3	.08 .22	7 5

In the evaluation of moment coefficients and, consequently, center
of pressure, there is an additional source of error introduced by the
transference of the moment as measured about the balance center of
moment to the desired point on the wing. The maximum error in individual
moment data points is believed to be as follows:

α, deg	Wing 2		Wing 5	
	ΔC_M	$\Delta C.P.$	ΔC_M	$\Delta C.P.$
2	0.0004	0.02	0.0004	0.05
5	.0008	.015	.0005	.02
10	.0017	.015	.0008	.01
15	.0026	.015	.0012	.01

The forces as measured include the force due to the sting support,
interference effects of the support, and base- and balance-pressure
effects on the support. Corrections due to the lift and drag of the
support sting were applied to the coefficients utilizing the forces on
similar stings tested without wings. No attempt was made to determine
the interference effects between sting and wing. They are believed to
be small since the area affected by the shocks from the sting is small
and the pressure rise due to sting is believed to be small. The pressures
at the base of the sting and in the balance were different when a

sting-mounted wing was tested than when a tare sting was tested; there-
fore, a correction was made to the total drag coefficient to account for
this pressure difference.

RESULTS AND DISCUSSION

Lift and Drag Characteristics

Figure 2 presents the lift and drag coefficients and the lift-drag
ratio as a function of angle of attack for the wings tested. The solid
lines are the values of these parameters predicted for the airfoil sec-
tion (in the streamwise direction) by the two-dimensional shock-expansion
theory (see table II), whereas the dashed lines are the wing coefficients
obtained from the Newtonian impact theory (appendix A). The same value
of skin-friction coefficient has been added to the pressure-drag coeffi-
cient from both the shock-expansion and impact theories, the skin-friction
coefficient being estimated as given in a later section concerning the
drag at zero angle of attack.

Lift coefficient as a function of angle of attack.- The lift coeffi-
cients of the wing having a semiapex angle of 30° (fig. 2(a)) are close
to the predictions of the two-dimensional shock-expansion theory at very
low angles of attack, but are more than twice as great as the predictions
of the Newtonian impact theory. As the angle of attack is increased, the
experimental values of lift coefficient drop markedly below the predic-
tions of shock-expansion theory. The angle of attack at which the lift
values begin to fall below the predictions of the shock-expansion theory
is only slightly less than the theoretically predicted shock-detachment
angle. (See apendix B.) This is in general agreement in this respect
with data obtained on thin delta wings at Mach numbers of 4 and 6.86
(ref. 7).

As the semiapex angle is decreased, the lift coefficients at any
given angle of attack decrease still further below the shock-expansion
theory (figs. 2(b) to 2(e)) and approach the values predicted by the
Newtonian theory. Whether or not the Newtonian theory can be expected
to give a lower limit for the lift of these wings at arbitrarily high
Mach numbers will be considered later.

In order to show more readily the change in the experimental C_L
for the various semiapex angles in comparison to the values of C_L
predicted by the two-dimensional shock-expansion theory, as a function
of angle of attack, figure 3 has been prepared. In addition, the ratio
given by the Newtonian impact theory between the lift for delta wings
and the two-dimensional lift has been included in figure 3 (calculated
as shown in appendix A). The decrease in the experimental values of C_L

below that given by the two-dimensional shock-expansion theory as the semiapex angle is decreased is quite marked. As α approaches zero for the wing with $\epsilon = 30^O$, the experimental C_L approaches that given by two-dimensional shock-expansion theory; however, at $\alpha = 16^O$ it is about 20 percent below that given by shock-expansion theory. For the wing with the highest sweep, $\epsilon = 5^O$, the experimental C_L is about 63 percent below the shock-expansion values at very low α and about 45 percent below at $\alpha > 15^O$. It is interesting to compare the results of the calculations based on the Newtonian theory with the experimental results presented in figure 3. The wings with the largest apex angles, $\epsilon = 30^O$ and 22°, in addition to having the experimental results poorly predicted by the Newtonian theory, have a different trend than is given by the theory. The wings with semiapex angles less than 22° can be said to have their trends predicted in a qualitative sense though quantitatively the prediction is poor.

Slope of the lift curves at zero angle of attack.- As a starting point for exploring the possibility of predicting the lift of these wings, the lift-curve slopes at 0° angle of attack will be studied according to parameters suggested by the linear theory. The initial lift-curve slope can also be an important consideration in certain stability problems.

According to linear theory, if the ratio of the lift-curve slopes at zero angle of attack of delta wings to the two-dimensional lift-curve slope are plotted as a function of $\tan \epsilon/\tan m$ the results will correlate on a given single curve. The wings of this investigation, 8 percent thick with the maximum thickness forward at the 18-percent-chord point, cannot be considered thin in the sense of the linear theory even at relatively low supersonic Mach numbers as shown by Love (ref. 13) in tests of delta wings with this section at Mach numbers in the range 1.62 to 2.40; however, Love did find that his data correlated on essentially a single curve though not that given by the linear theory. The data of Love and that of the present investigation are presented in figure 4. The two-dimensional lift-curve slope used to nondimensionalize all the data on this figure is that given by the shock-expansion theory which was shown in reference 7 to give good results for thin wings. The good correlation of Love's data is quite evident.

The data for $M = 2.40$ show an increase in lift-curve-slope ratio as the tangent ratio ($\tan \epsilon/\tan m$) increases, apparently approaching a value of 1 at a value of the tangent ratio near that for shock attachment. Though the data shown for $M = 1.62$ and 1.92 correlate well with the 2.40 data, it must be pointed out that the data for the lower Mach numbers have not been carried to a high enough value of tangent ratio to determine whether or not they will diverge from the $M = 2.40$ data at some point and approach their respective shock-attachment points shown on figure 4.

The data obtained in the present investigation at $M = 6.9$ do not correlate with the data of reference 13 though these data do exhibit similar characteristics. At a value of the tangent ratio greater than that for shock detachment the lift ratio is close to 1; at values of the tangent ratio less than that for shock attachment the lift ratio apparently decreases abruptly from its value near 1 with the general shape of the curve in this region being somewhat similar to Love's for $M = 2.40$.

It is obvious that for wings such as these the method devised by Ulmann and Bertram (ref. 7) for predicting the zero angle-of-attack lift-curve slope cannot be applied since it is based on the linear theory and is thus restricted to thin wings where the tangent ratio for shock attachment is reasonably close to a value of one.

Since correlations for the data at $M = 6.9$ with lower Mach number data based on the usual parameters suggested by linear theory are not feasible, it was deemed advisable to compare the data on the basis of other variables which would allow a more direct assessment of the Mach number effects, which are obviously large at high Mach numbers. Thus, figure 5 was prepared in which the zero angle-of-attack lift-curve slope is presented as a function of the reciprocal of the Mach number.[1] Included in this figure are data at Mach numbers from 1.62 to 2.40 (ref. 13), unpublished data obtained at $M = 4.04$ in the Langley 9- by 9-inch Mach number 4 blowdown jet, and data from the present tests at $M = 6.9$.

For semiapex angles of $22°$ or greater the data form a family of essentially similar curves with the data for a given ϵ approaching the curve given by the two-dimensional shock-expansion theory as the Mach number is increased and attaching to it at a Mach number slightly higher than that indicated for shock attachment. The shock attachment values, however, serve as a guide for the proper fairing of the data. The shock-expansion theory was evaluated to a Mach number of 40 assuming the ratio of the specific heats to be invariant at a value of 1.4, the dashed portion of this curve on figure 5 indicates values extrapolated from $M = 40$ to $M = \infty$. The lift-curve slope given by shock-expansion theory from $M = \infty$ is, as expected, considerably higher than that given by the two-dimensional Newtonian theory.

In the actual case, however, the values of the aerodynamic coefficients at extremely high Mach numbers can be expected to approach more nearly the Newtonian theory than the shock-expansion theory, with $\gamma = 1.4$, since at extremely high Mach numbers the area affected by shocks

---

[1]Linear theory suggests $1/\sqrt{M^2 - 1}$ as an abscissa and for thin wings this parameter might be used to good advantage but has no advantage over the reciprocal of the Mach number for the thick wings used in this investigation.

from the surface becomes a thin film on the surface with an extremely
large temperature rise where the ordinary assumptions of flow without
conduction or radiation would no longer apply. (See Epstein, ref. 16,
and Laitone, ref. 17.) Additional deviations from the shock-expansion
theory as the Mach number becomes very large might be expected if one
considers the case where the viscous flow fills the space between the
surface and the shock wave, and shock-boundary-layer interaction becomes
important. (See Shen, ref. 18.)

Below a semiapex angle of 22° (between $\epsilon = 22^O$ and $\epsilon = 17.9^O$) a
decided change occurs in the trends of the experimental data at the higher
Mach numbers. The data for $\epsilon = 17.9^O$ apparently are not defined by this
wing's shock-attachment point as the Mach number approaches the value that
is theoretically indicated to be that for shock attachment. Instead, the
lift-curve slope appears to approach more nearly as a limit the value
given by the Newtonian impact theory. This appears also to be the case
for $\epsilon = 9.93^O$. (The dashed portion of the curve for $M < 6.9$ for
$\epsilon = 5^O$ was obtained from an extrapolation of the data from reference 13
and the Langley 9- by 9-inch Mach number 4 blowdown jet and is intended
to serve as a guide for the approximate values of $(dC_L/d\alpha)_0$ to be
expected in this region.) For the more highly swept wings, then, it
appears that the wing geometry is such that shock attachment does not
have any decided effect upon the trend of the lift-curve slope with Mach
number. This apparent disappearance of the effect of shock attachment
would be expected to manifest itself at still larger ϵ as the angle of
attack increases.

Drag coefficient as a function of angle of attack.- For the drag
coefficient at angle of attack much the same comments apply as for the
lift coefficient considered previously. For a semiapex angle of 30°
(fig. 2(a)) at very low angles of attack the drag coefficient is close
to the prediction given by shock-expansion theory. As the angle of attack
is increased the experimental values of C_D drop markedly below the
theory. As the semiapex angle is decreased, the drag coefficient at any
given angle of attack is decreased still further below the shock-expansion
theory (figs. 2(b) to 2(e)) and approaches the Newtonian impact theory.

Drag coefficient at zero angle of attack.- An examination of the
drag coefficient at zero angle of attack as a function of Reynolds number
(fig. 6) indicates that its variation is consistent with the assumption
of a laminar boundary layer. At a given Reynolds number the drag coef-
ficients of the wings with $\epsilon = 30^O$ and $\epsilon = 22^O$ are practically equal
while with ϵ decreasing below 22° the drag decreases, the variation of
drag coefficient with Reynolds number being essentially unchanged.

For the wings with $\epsilon = 22^O$ and 30° the shock-expansion wave drag
plus an estimated laminary skin-friction coefficient represents the exper-
imental data with good accuracy over the range of test Reynolds numbers
(0.8×10^6 to 2.7×10^6).

At this point it might be well to give the method of estimating the skin-friction coefficients used in this report. For a triangular flat plate at zero angle of attack where the boundary layer formed on the plate is laminar, it can be shown that the effective chord for obtaining the average skin-friction coefficient of the plate is one-fourth of the root chord. Under the conditions of the present tests ($M = 6.9$ and $T_0 = 1130^\circ$ R) and using the results given by Bertram in reference 19 for an insulated flat plate

$$C_f = \frac{4.89}{\sqrt{R}} \tag{1}$$

where R is the Reynolds number based on root chord. For the front surfaces of the highly swept wings the flow in the boundary layer can be considered to be more conical in nature than two dimensional. Assuming the flow to be conical over the entire wing where the Reynolds number on the wing is equivalent to that in the free stream for the same length, a constant is obtained which differs from that given in equation (1) resulting in the following relation

$$C_f = \frac{4.44}{\sqrt{R}} \tag{2}$$

Equation (1) was used in estimating C_f for wings 1, 2, and 3, whereas an average between equations (1) and (2) ($C_f\sqrt{R} = 4.66$) was used for wings 4 and 5.

Using these estimated skin-friction coefficients the inviscid zero-angle drag coefficients were found for the data at $M = 6.9$. The inviscid zero-angle-of-attack drag-coefficient data at Mach numbers from 1.62 to 2.40 were obtained from reference 7 where the data presented in reference 13 were corrected for skin friction with the assumption that the boundary layer was laminar up to the ridge line and turbulent after the ridge line. These values have been divided by the values from shock-expansion theory and are presented in figure 7 as a function of tangent ratio, the same parameter previously used to present lift-curve-slope data (fig. 4). The present data at $M = 6.9$ do not correlate with that at the lower supersonic Mach numbers. The discrepancy between the two sets of data is too large to be explained on the basis of incorrect estimates of skin friction.

With similar reasoning to that used for the zero-angle-of-attack lift-curve slope the inviscid drag coefficients at zero angle of attack are presented as a function of the reciprocal of the Mach number in figure 8. Again, this figure includes data at Mach numbers from 1.62 to 2.40 (ref. 13), as shown in figure 7, unpublished data obtained in the

Langley 9- by 9-inch Mach number 4 blowdown jet at $M = 4.04$, and data
from the present tests at $M = 6.9$. Much the same effects as were found
in the case of lift-curve slope (fig. 5) are shown by the drag data.
Again, for semiapex angles of $22°$ or greater, the data form a family of
essentially similar curves with the data for a given semiapex angle
approaching the curve given by the two-dimensional shock-expansion theory
and attaching to it at about the Mach number theoretically indicated for
shock attachment.

The shock-expansion theory was evaluated to a Mach number of 40
($\gamma = 1.4$). The dashed portion of the curve for shock-expansion theory
between $M = 40$ and $M = \infty$ on figure 8 indicates extrapolated values.
The zero-angle drag coefficient given by shock-expansion theory for
$M = \infty$ appears to be higher than that given by the two-dimensional
Newtonian theory. It should be pointed out that expansion waves from
the model surface reflected from the bow shock of the two-dimensional
wing strike the rear surface at the lower supersonic Mach numbers. At
$M = 1.62$ the first wave strikes the body at the 79-percent-chord point.
For such a condition the shock-expansion solution is not exactly equiva-
lent to the characteristics solution.

Below a semiapex angle of $22°$ (between $\epsilon = 22°$ and $\epsilon = 17.9°$)
there is a change in the tendencies of the data. As the Mach number
approaches the Mach number that is theoretically indicated to be that
for shock attachment the data for $\epsilon = 17.9°$ apparently are not defined
by its shock-attachment point. Instead, this curve and that for $\epsilon = 9.9°$
approach, as a limit, a value that may be approximately given by the
Newtonian theory. The dashed portion of the curve for $\epsilon = 5°$ at
$M < 6.9$ was obtained from an extrapolation of the data from reference 13
and the Langley 9- by 9-inch Mach number 4 blowdown jet and is intended
to serve as a guide for the approximate value of $C_{D_{0_i}}$ to be expected
in this region.

Variation of the chord-force coefficient with angle of attack.-
Measurements of C_C were made on all the wings at low angles of attack
and these data are presented in figure 9 as the ratio of the change in
chord force from the value at zero angle of attack to the inviscid zero-
angle drag coefficient as a function of angle of attack. In the two-
dimensional case shock-expansion theory indicates an increase in C_C with
α and the experimental values from the wing with $\epsilon = 30°$ agree with
this predicted increase. However, for $\epsilon = 22°$ a decrease in C_C below
the zero angle-of-attack value was found with increasing α and for still
smaller ϵ further decreases were found.

Impact theory indicates that C_C will decrease below C_{D_0} as ϵ
decreases; still, the decrease shown experimentally occurs at a much lower
angle of attack than does the decrease based on impact considerations.
Part of the decrease may be attributed to wing geometry (as indicated by

impact theory) but other factors must also be present. Changes in skin
friction with angle of attack cannot be expected to account for the
decrease in C_C that have been measured. Ordinarily the skin friction
is expected to increase with angle of attack. The often discussed leading-
edge suction comes to mind in this regard but nothing definite can be
stated at the present time.

Lift-drag ratio.- The experimental lift-drag ratios of the wings
having semiapex angles of 30° and 22° (figs. 2(a) and 2(b)) agree very
well with the predictions of the two-dimensional shock-expansion theory.
However, at the higher angles of attack this agreement occurs because the
experimental lift and drag coefficients are both lower than the theoreti-
cal predictions by approximately equal percentages. The experimental
lift-drag ratios for the wings having semiapex angles of 9.93^O and 5°
(figs. 2(d) and 2(e)) are considerably greater than those obtained from
shock-expansion theory assuming the same estimated skin friction, and
the agreement with the predictions of Newtonian theory is also poor.

Earlier it has been stated that the Newtonian theory predicts large
decreases in chord-force coefficient for these wings at angles of attack
above 2.79^O. These decreases result in the increases in the lift-drag
ratio which are indicated in figure 10. The increases in lift-drag ratio
are rapid as ϵ is increased below about 18°. In order to compare the
experimentally obtained increases in L/D with those predicted by the
Newtonian theory, the shock-expansion theoretical values of L/D were
increased by the ratio of the three-dimensional Newtonian L/D to the
two-dimensional Newtonian L/D given in figure 10. This comparison is
shown in figure 11 for wings 3, 4, and 5 ($\epsilon = 17.91^O$, 9.93^O, and 5°).
Wings 1 and 2 are not included, since Newtonian theory (fig. 10) alters
the two-dimensional lift-drag ratio only slightly. An estimated skin-
friction drag coefficient (shown in fig. 2) has been subtracted from the
experimental results. The trend of this modification to shock-expansion
theory is seen to be approximately correct, but for the wing having
$\epsilon = 5^O$ the experimental value of maximum L/D is displaced from that
given by the theory. The reason for this is apparent from an examination
of the experimental chord-force data (fig. 9) and the chord-force coef-
ficients obtained from impact theory. Experimentally, where a decrease
in chord force occurs, it starts at zero angle of attack and continuously
decreases to an angle of attack between 6° to 8° while from impact theory
the decrease in chord force (with its associated increase in L/D
(fig. 10)) only begins when the bottom rear surface becomes exposed to
the stream, that is above an angle of attack of 2.79^O.

Lift-drag ratio as a function of lift coefficient.- In order to show
the relative merits of these wings on a lift-drag basis the wings have
been compared assuming constant area (shown in fig. 12). Several bases
of comparison are possible and the constant-area assumption was chosen
as having the advantage of simplicity in addition to being a logical means

of comparison. Up to lift coefficient of 0.1 the L/D of the wings
increases with decreasing ε. Above this lift coefficient the wings with
the smallest ε appear to have a slightly lower L/D than those with
say, ε = 30° and ε = 22°. The variation of L/D with C_L is pre-
dicted rather well by the modified shock-expansion theory, with the
exception of the wing with ε = 5°, up to a value of C_L of about 0.08,
above which value of C_L the modified shock-expansion theory overesti-
mates the value of L/D associated with a given value of C_L by about
10 percent. This agreement might be expected to improve at still higher
Mach numbers.

The fact that for this comparison the data had to be corrected to a
Reynolds number other than that at which the tests were conducted is
believed to introduce only negligible errors since the total friction
coefficient is not a large part of the drag coefficient and only a small
correction was required to the friction coefficient. Also the change in
skin friction computed theoretically was in agreement with the experimen-
tally determined effect of varying the Reynolds number.

These results may be compared to results obtained for bodies such
as those reported by Ridyard in reference 20. In this reference, cone
cylinders and bodies with D-shape cross sections were tested at M = 6.86.
Since there is a general increase in the efficiency of bodies with
increasing Mach number they can be expected to provide much or all of
the lift required in hypersonic flight. On the other hand the more highly
swept wings might be considered to perform the functions of bodies though
the wings considered here were not chosen for their efficiency in hyper-
sonic flight. When compared with the results from reference 20 all of
the wings are found to be more efficient than the 10° cone cylinders
except for the wings with the larger apex angles at low lift coefficients.
The body designated as D-body 2 gave results equivalent to those from
the wing with ε = 9.93°. D-body 3 of reference 20 might be considered
somewhat better than the wing with ε = 5° since the maximum lift-drag
ratio for the body, which is about equal to that for the wing, occurs at
a higher lift coefficient. In general, for values of C_L greater than
that at which (L/D)$_{max}$ occurs the values of L/D obtained for D-body 3
are slightly greater than or equal to (at large C_L) those for any of the
wings tested. The difference in Reynolds number between the results of
the present tests and those reported in reference 20 are not large and
therefore are not believed to be important for this comparison.

Center of Pressure and Moment Coefficient

As shown in figure 13, moment data indicate the center of pressure
to be close to the center of area for the two wings for which such data
were obtained. For ε = 22° the center of pressure was within 10 per-
cent (ahead) of the center of area varying somewhat with α (in the

range 0° to 12°), while for the wing with $\epsilon = 5^O$ the center of pressure was essentially at the center of area (within the data accuracy) over the range of angle of attack from 0° to 21°. Love (ref. 13) in tests of these wings at Mach numbers between 1.6 and 2.4 also found the center of area and the center of pressure to be practically coincident.

Schlieren Photographs

Figures 14 to 17 present schlieren photographs taken during the course of this investigation. These schlieren photographs illustrate the shock patterns about the wings. The side views (figs. 14, 16, and 17) show that the shock from the under surface becomes essentially parallel to the chord line at about $\alpha = 20^O$ for the wing with $\epsilon = 5^O$ and at higher angles of attack for the other wings. The side views of wings 4 and 5 in figures 16(c) and 17 show the shock to be lying essentially along the ridge line at the front of the wing.

For wing 2 ($\epsilon = 22^O$) theory indicates that the shock is just at the detachment point at $\alpha = 0$. The schlieren photographs of this wing taken with a top view (fig. 15) appear to substantiate this, the visible disturbance leaving the wing at its very tip at $\alpha = 0$. As α increases the shock moves away from the leading edge. The top view schlieren photograph of wing 5 ($\epsilon = 5^O$), figure 17(a), at essentially $\alpha = 0$ shows a weak shock standing at an angle of about 5° from the wing leading edge.

Surface Film Flow Studies

Oil flow studies on the surface of wings 2 and 5 ($\epsilon = 22^O$ and 5°) (the results of which are shown in figs. 18 and 19) were made by viewing the patterns made by the fluorescing oil during a run.

The results from the lower surface of wing 2 (figs. 18(c) and 18(e) and other pictures) indicate the surface flow is essentially parallel to the free-stream flow. At $\alpha = 6.9^O$ aside from the area affected by the shock from the sting there is an indication of a disturbance starting just behind the thickness peak and extending out as a ray on either side of the center line. This disturbance, however, does not appear to affect much of the area of the lower surface. At $\alpha = 18.8^O$ on the lower surface the flow lines are similar to those experienced at $\alpha = 6.9^O$; however, there appears to be a short length of flow separation lying along the ridge line as shown by the accumulation of oil just behind the ridge line.

On the upper surface of wing 2 (figs. 18(b), (d), and (f)) the flow phenomena appear to be somewhat more complicated. In general, for all the angles of attack investigated there is an expansion around the ridge

line after which the flow separates. A shock probably is present where the separation occurs. The line of flow separation moves closer to the ridge line as the angle of attack increases; the separated flow apparently reattaches to the surface farther towards the wing center line, curling under and moving toward the trailing edge. The rays indicating flow separation and reattachment apparently have their origin at the maximum thickness location. This flow phenomenon considered is apparently compatible with the theoretical concept advanced by Brown and Micheals (ref. 21). In addition to this flow there appears to be a separation emanating from the trailing edge of wing 2 which has a weak flow at the surface counter to the stream flow which moves forward to cover more of the upper rear surface as the angle of attack increases. In addition to the leading edge, a region of high shear is found along the center of the upper rear surface at all angles of attack investigated. Also, a disturbance is found at the wing tip covering only a small area which appears to be distinct from the other disturbances discussed. The schlieren photographs corresponding to those of the surface fluid flow studies are shown in figure 15.

The flow patterns obtained on the upper surface of wing 5 ($\epsilon = 5°$), figure 19, appear to be roughly similar in the general location and movement of the rays shown by the oil accumulations to those obtained from wing 2. These rays again apparently have their origin at the point of maximum thickness. Again a high shear region is found lying along the center line of the upper rear surface but this region occupies a much greater proportion of the wing area as compared to wing 2. Separation near the trailing edge appears to start at the tip moving in toward the center line and affecting more of the wing as the angle of attack increases. The bright area at the visible forward part of wing 5 in figure 19(b) is caused by reflected light and does not indicate an oil accumulation.

The effects found on the upper rear surface of wings 2 and 5 appear to be roughly similar to those found at lower supersonic Mach numbers. for example, the work of Love (ref. 13), Boyd and Phelps (ref. 22), Hatch and Gallagher (ref. 23), and Love and Grigsby (ref. 24). The investigation reported in references 22 and 23 was made with thin delta wings with rounded and sharp leading edges in the Mach number range between 1.2 and 1.9. For various reasons a detailed comparison to these results is not feasible.

SUMMARY OF RESULTS

A program to investigate the aerodynamic characteristics of a family of delta wings with a blunt double-wedge section has been conducted at the Langley 11-inch hypersonic tunnel at a Mach number of 6.9. These

wings had a maximum thickness of 8 percent of the chord located at the 18-percent-chord point. The semiapex angle of the wings was varied from 30° down to 5° and the wings were tested over a range of angle of attack from 0° to 28° and Reynolds numbers in the range of 0.8×10^6 to 3.6×10^6 based on root chord. An analysis of the results of this investigation and comparisons with existing data for wings of the same family at lower supersonic Mach numbers have led to the following observations.

1. The lift and drag coefficients lay in the region bounded by the two-dimensional shock-expansion theory and the Newtonian impact theory.

2. The parameters suggested by the linear theory are not of any aid in correlating the data at high supersonic Mach numbers, that is, Mach numbers above about 3.

3. Consideration of the available data for these wings at Mach numbers between 1.62 and 6.9 indicates that when the leading-edge shock wave is detached the drag and lift-curve slope at zero angle of attack for a given semiapex angle tend toward the values given by two-dimensional shock-expansion theory with increasing Mach number when the semiapex angle is equal to or greater than 22°. For semiapex angles less than 22° the data indicate that the trend with increasing Mach number is to approach the approximate value for the particular wing given by the impact theory. For the more highly swept of these wings, then, it appears that the wing geometry is such that shock attachment does not have any decided effect upon the trend of the lift-curve slope and drag at zero angle of attack with Mach number.

4. The lift-drag ratio increases with decreases in semiapex angle mainly because of a rapid decrease in chord force as the angle of attack increased.

5. The moment data indicate the center of pressure to be close to the center of area for the two wings for which such data were obtained (semiapex angles of 22° and 5°).

6. Surface film flow studies indicate the presence of shocks on the upper rear surface roughly similar to those found at lower supersonic Mach numbers.

Langley Aeronautical Laboratory,
        National Advisory Committee for Aeronautics,
                Langley Field, Va., July 12, 1954.

APPENDIX A

THE NEWTONIAN IMPACT THEORY APPLIED TO DELTA WINGS

WITH DOUBLE-WEDGE SECTIONS
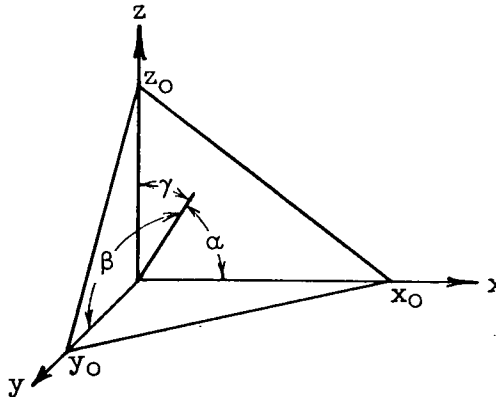
In order to obtain the orientation of a plane surface with respect to a flowing gas, consider the plane whose intercepts are x_O, y_O, and z_O. The intercept equation gives

$$\frac{x}{x_O} + \frac{y}{y_O} + \frac{z}{z_O} = 1$$

The direction cosines to the plane are[1]

$$\cos \alpha = - \frac{1/x_O}{\sqrt{\frac{1}{x_O^2} + \frac{1}{y_O^2} + \frac{1}{z_O^2}}} \tag{A1}$$

$$\cos \beta = - \frac{1/y_O}{\sqrt{\frac{1}{x_O^2} + \frac{1}{y_O^2} + \frac{1}{z_O^2}}} \tag{A2}$$

---

[1]The symbol α in this appendix is used to designate the direction angle from the x-axis of the normal to the plane as is conventional while α'' will be used to designate wing angle of attack. In the main body of the report α designates wing angle of attack.

$$\cos \gamma = - \frac{1/z_0}{\sqrt{\dfrac{1}{x_0{}^2} + \dfrac{1}{y_0{}^2} + \dfrac{1}{z_0{}^2}}} \tag{A3}$$

From equations (A1) and (A2)

$$\cos \alpha = \pm \frac{\sin \beta}{\sqrt{1 + \left(\dfrac{x_0}{z_0}\right)^2}} \tag{A4}$$

And combining equations (A2) and (A3)

$$\cos \gamma = \pm \frac{\sin \beta}{\sqrt{1 + \left(\dfrac{z_0}{x_0}\right)^2}} \tag{A5}$$

If the surface under consideration is the front plane of a swept wing with the line $x_0 - z_0$ designating the front ridge line (flow parallel to the x axis) then the direction angle β is designated solely by the wing geometry. In this case with ϵ the semiapex angle of the wing, a the location of the ridge line termination in a fraction of the chord length, c the chord length, and t twice the thickness at the ridge-line termination (measured from and normal to the chord line) there is obtained

$$\sin \beta = \frac{1}{\sqrt{1 + \dfrac{(t/ac)^2}{\tan^2\epsilon\,(4 + (t/ac)^2)}}} \tag{A6}$$

and since x_0/z_0 is determined by the position of the ridge line

$$1 + \left(\frac{x_0}{z_0}\right)^2 = \frac{(1 + \cot^2\alpha'')\left[1 + \left(2a\,\dfrac{c}{t}\right)^2\right]}{\left(\cot \alpha'' \mp 2a\,\dfrac{c}{t}\right)^2} \tag{A7}$$

where α'' is the angle of attack measured from the chord line. Thus, substituting equations (A6) and (A7) into equations (A4) and (A5)

$$\cos \alpha = \frac{\frac{t}{2ac} \cos \alpha'' \mp \sin \alpha''}{\left[1 + \left(\frac{t}{2ac \ \sin \ \epsilon} \right)^2 \right]^{1/2}} \tag{A8}$$

and

$$\cos \gamma = \frac{\cos \alpha'' \pm \frac{t}{2ac} \sin \alpha''}{\left[1 + \left(\frac{t}{2ac \ \sin \ \epsilon} \right)^2 \right]^{1/2}} \tag{A9}$$

In equations (A7), (A8), and (A9) where a dual sign is indicated the upper sign is used where the upper surface is being considered and the lower sign where the lower surface is under consideration.

Now, the Newtonian impact theory assumes that the force acting on a surface is due to the inelastic impact of the fluid mass which impinges on the surface. Thus, in our notation the normal-force coefficient (that is, normal to the surface) for a front surface of a swept wing, for which the direction angles of equations (A8) and (A9) have been obtained, is

$$C_{N_f} = 2 \cos^2 \alpha \ \frac{S_f}{S_p} \tag{A10}$$

where S_f is the area of the surface and S_p is the total plan-form area of the wing. Considering now a triangular plan-form wing with a double-wedge airfoil where S_f is the true area of a front surface

$$\frac{S_f}{S_p} = a \sqrt{1 + \left(\frac{t}{2ac \ \sin \ \epsilon} \right)^2} \tag{A11}$$

The lift and drag coefficients of this front surface are

$$C_{L_f} = 2a \cos^2 \alpha \ \cos \gamma \sqrt{1 + \left(\frac{t}{2ac \ \sin \ \epsilon} \right)^2} \ . \tag{A12}$$

$$C_{D_f} = 2a \cos^3 \alpha \sqrt{1 + \left(\frac{t}{2ac \ \sin \ \epsilon} \right)^2} \tag{A13}$$

and with equations (A8) and (A9)

$$C_{L_f} = \frac{2a}{1 + \left(\dfrac{t}{2ac\ \sin\ \epsilon}\right)^2}\left(\frac{t}{2ac}\cos\ \alpha'' \mp \sin\ \alpha''\right)^2\left(\cos\ \alpha'' \pm \frac{t}{2ac}\sin\ \alpha''\right) \quad (A14)$$

$$C_{D_f} = \frac{2a}{1 + \left(\dfrac{t}{2ac\ \sin\ \epsilon}\right)^2}\left(\frac{t}{2ac}\cos\ \alpha'' \mp \sin\ \alpha''\right)^3 \quad (A15)$$

again where a dual sign occurs the upper one is used for the upper surface and the lower one for the lower surface.

Since the lee surfaces do not contribute to the forces on a wing or body from impact considerations, if the airfoil considered is a double wedge then at most one of the rear surfaces can contribute to the aerodynamic forces at any given attitude. (At the lower angles of attack both rear surfaces can be shielded from the flow and thus would not contribute at all to the aerodynamic forces.) So far as impact theory is concerned the rear surfaces of a double-wedge section triangular plan-form wing are two dimensional and the coefficient for the force normal to the surface is

$$C_{N_r} = 2\ \sin^2(\alpha'' - \lambda_2)\ \frac{S_r}{S_p} \quad (A16)$$
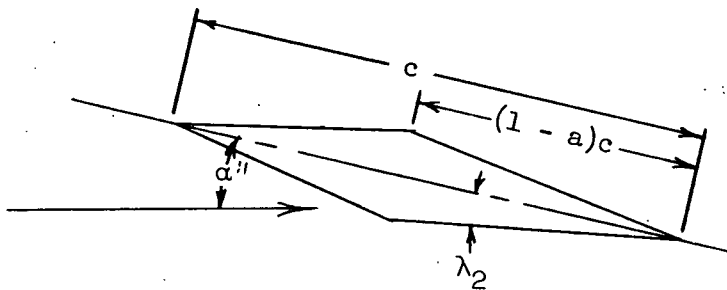
The ratio of the area of the rear surface to the plan-form area is

$$\frac{S_r}{S_p} = (1 - a)\sqrt{1 + \left(\frac{t}{2(1 - a)c}\right)^2} \quad (A17)$$

The lift and drag coefficients of the rear surface are

$$C_{L_r} = 2(1 - a)\sqrt{1 + \left(\frac{t}{2(1 - a)c}\right)^2} \sin^2(\alpha'' - \lambda_2) \cos(\alpha'' - \lambda_2) \quad \text{(A18)}$$

$$C_{D_r} = 2(1 - a)\sqrt{1 + \left(\frac{t}{2(1 - a)c}\right)^2} \sin^3(\alpha'' - \lambda_2) \quad \text{(A19)}$$

Since

$$\sin(\alpha'' - \lambda_2) = \frac{\sin \alpha'' - \dfrac{t}{2(1 - a)c} \cos \alpha''}{\sqrt{1 + \left(\dfrac{t}{2(1 - a)c}\right)^2}} \quad \text{(A20)}$$

and

$$\cos(\alpha'' - \lambda_2) = \frac{\cos \alpha'' + \dfrac{t}{2(1 - a)c} \sin \alpha''}{\sqrt{1 + \left(\dfrac{t}{2(1 - a)c}\right)^2}} \quad \text{(A21)}$$

the expressions for C_{L_r} and C_{D_r} are

$$C_{L_r} = \frac{2(1 - a)}{1 + \left(\dfrac{t}{2(1 - a)c}\right)^2}\left(\sin \alpha'' - \frac{t}{2(1 - a)c} \cos \alpha''\right)^2\left(\cos \alpha'' + \right.$$

$$\left. \frac{t}{2(1 - a)c} \sin \alpha''\right) \quad \text{(A22)}$$

and

$$C_{D_r} = \frac{2(1 - a)}{1 + \left(\dfrac{t}{2(1 - a)c}\right)^2}\left(\sin \alpha'' - \frac{t}{2(1 - a)c} \cos \alpha''\right)^3 \quad \text{(A23)}$$

The surfaces involved at any given angle of attack will depend on the value of a for the upper and lower surfaces. Depending on the value of a and the angle of attack, in treating one-half of the wing anywhere from one to three surfaces can be involved.

It should be pointed out that these equations can be easily adapted for the determination of the force coefficients for an airfoil that is nonsymmetrical about the chord, that is, for a double-wedge airfoil which has different values of a and t/c for the top and bottom surfaces.

APPENDIX B

SHOCK DETACHMENT

The symbols used in this appendix are as follows:

M_1 Mach number in free-stream flow direction

M_2 resultant Mach number normal to leading edge

γ ratio of specific heats C_p/C_v

f a function of Mach number

δ_m maximum deflection angle for shock attachment

ϵ semiapex angle

ϵ_m minimum semiapex angle for shock attachment

α angle of attack

α_m maximum angle of attack for shock attachment

λ_1 angle at leading edge of a section taken in free-stream direction
      and in a plane perpendicular to plan form measured from chord
      line

m_1 Mach angle based on M_1

In order to determine the point of shock detachment for the tri-
angular plan-form wings under consideration the following procedure is
used.

For the determination of the semiapex angle for shock detachment
at a given angle of attack

$$\sin \epsilon_m = \frac{\cot \delta_m}{2}(\tan \alpha + \tan \lambda_1) +$$

$$\sqrt{\tan \alpha \tan \lambda_1 + \left[(\tan \alpha + \tan \lambda_1)\frac{\cot \delta_m}{2}\right]^2} \qquad (B1)$$

and

$$M_1 = \frac{M_2}{\sqrt{1 - \cos^2\alpha \, \cos^2\epsilon_m}} \qquad (B2)$$

where actually equation (B2) holds for all values of ϵ including ϵ_m. Cot δ_m is a function only of M_2 and can be obtained from

$$\cot \delta_m = \frac{\frac{\gamma}{f}\left(1 + \frac{\gamma + 1}{2} M_2^2\right) - 1}{\left(1 - \frac{\gamma}{f}\right)\sqrt{\frac{\gamma}{f} M_2^2 - 1}} \qquad (B3)$$

where

$$f = \left(\frac{\gamma + 1}{4} M_2^2 - 1\right) + \sqrt{(\gamma + 1)\left(1 + \frac{\gamma - 1}{2} M_2^2 + \frac{\gamma + 1}{16} M_2^4\right)}$$

which at infinite Mach number becomes $\cot \delta_m = \sqrt{(\gamma - 1)(\gamma + 1)}$. With $\gamma = 1.4$ tabulated values, such as those from reference 25, can be used to obtain δ_m as a function of M_2.

Since equations (B1) and (B2) are interdependent, they were solved by assuming various values of M_2, thus giving values of M_1. The desired value of M_1 was obtained by graphical interpolation of the computed values.

To determine the angle of attack for shock detachment for a given semiapex angle the following equation is used:

$$\tan \alpha_m = \sin \epsilon \left(\frac{\sin \epsilon - \cot \delta_m \tan \lambda_1}{\sin \epsilon \cot \delta_m + \tan \lambda_1}\right) \qquad (B4)$$

Here again values of M_2 can be assumed and the corresponding M_1 determined from equation (B2).

For zero angle of attack the tangent ratio for shock detachment can be obtained easily from the relation

$$\frac{\tan \epsilon_m}{\tan m_1} = \tan \lambda_1 \cot \delta_m \sqrt{\frac{M_1^2 - 1}{1 - (\tan \lambda_1 \cot \delta_m)^2}} \qquad (B5)$$

REFERENCES

1. McLellan, Charles H., Bertram, Mitchel H., and Moore, John A.: An
   Investigation of Four Wings of Square Plan Form at a Mach Number
   of 6.86 in the Langley 11-Inch Hypersonic Tunnel. NACA RM L51D17,
   1951.

2. McLellan, Charles H.: Exploratory Wind-Tunnel Investigation of Wings
   and Bodies at M = 6.9. Jour. Aero. Sci., vol. 18, no. 10,
   Oct. 1951, pp. 641-648.

3. Ulmann, Edward F., and Lord, Douglas R.: An Investigation of Flow
   Characteristics at Mach Number 4.04 Over 6- and 9-Percent-Thick
   Symmetrical Circular-Arc Airfoils Having 30-Percent-Chord Trailing-
   Edge Flaps. NACA RM L51D30, 1951.

4. Ulman, Edward F., and Dunning, Robert W.: Aerodynamic Characteristics
   of Two Delta Wings at Mach Number 4.04 and Correlations of Lift and
   Minimum-Drag Data for Delta Wings at Mach Numbers From 1.62 to 6.9.
   NACA RM L52K19, 1952.

5. Dunning, Robert W., and Ulmann, Edward F.: Aerodynamic Characteristics
   at Mach Number 4.04 of a Rectangular Wing of Aspect Ratio 1.33 Having
   a 6-Percent-Thick Circular-Arc Profile and a 30-Percent-Chord Full-
   Span Trailing-Edge Flap. NACA RM L53D03, 1953.

6. Dunning, Robert W., and Smith, Fred M.: Aerodynamic Characteristics
   of Two Delta Wings and Two Trapezoidal Wings at Mach Number 4.04.
   NACA RM L53D30a, 1953.

7. Ulmann, Edward F., and Bertram, Mitchel H.: Aerodynamic Characteris-
   tics of Low-Aspect-Ratio Wings at High Supersonic Mach Numbers.
   NACA RM L53I23, 1953.

8. Puckett, Allen E.: Supersonic Wave Drag of Thin Airfoils. Jour. Aero.
   Sci., vol. 13, no. 9, Sept. 1946, pp. 475-484.

9. Robinson, A.: Lift and Drag of a Flat Delta Wing at Supersonic Speeds.
   Tech. Note No. Aero. 1791, British R.A.E., June 1946.

10. Stewart, H. J.: The Lift of a Delta Wing at Supersonic Speeds.
    Quarterly Appl. Math., vol. IV, no. 3, Oct. 1946, pp. 246-254.

11. Brown, Clinton E.: Theoretical Lift and Drag of Thin Triangular Wings
    at Supersonic Speeds. NACA Rep. 839, 1946. (Supersedes NACA
    TN 1183.)

12. Puckett, A. E., and Stewart, H. J.: Aerodynamic Performance of Delta
    Wings at Supersonic Speeds. Jour. Aero. Sci., vol. 14, no. 10,
    Oct. 1947, pp. 567-578.

13. Love, Eugene S.: Investigations at Supersonic Speeds of 22 Triangular
    Wings Representing Two Airfoil Sections for Each of 11 Apex Angles.
    NACA RM L9D07, 1949.

14. McLellan, Charles H., Williams, Thomas W., and Bertram, Mitchel H.:
    Investigation of a Two-Step Nozzle in the Langley 11-Inch Hyper-
    sonic Tunnel. NACA TN 2171, 1950.

15. McLellan, Charles H., Williams, Thomas W., and Beckwith, Ivan E.:
    Investigation of the Flow Through a Single-Stage Two-Dimensional
    Nozzle in the Langley 11-Inch Hypersonic Tunnel. NACA TN 2223,
    1950.

16. Epstein, Paul S.: On the Air Resistance of Projectiles. Proc. Nat.
    Acad. Sci., vol. 17, no. 9, Sept. 1931, pp. 532-547.

17. Laitone, Edmund V.: Exact and Approximate Solutions of Two-
    Dimensional Oblique Shock Flow. Jour. Aero. Sci., vol. 14, no. 1,
    Jan. 1947, pp. 25-41.

18. Shen, Shan-Fu: Hypersonic Flow Over An Insulated Wedge With Viscosity
    Effects. Part I. Sc. D. Thesis, M.I.T., 1949.

19. Bertram, Mitchel H.: An Approximate Method for Determining the Dis-
    placement Effects and Viscous Drag of Laminar Boundary Layers in
    Two-Dimensional Hypersonic Flow. NACA TN 2773, 1952.

20. Ridyard, Herbert W.: The Aerodynamic Characteristics of Two Series
    of Lifting Bodies at Mach Number 6.86. NACA RM L54C15, 1954.

21. Brown, C. E., and Micheal, W. H., Jr.: Effect of Leading Edge
    Separation on the Lift of a Delta Wing. Preprint no. 437,
    S.M.F. Fund Preprint, Inst. Aero. Sci., Inc., Jan. 1954.

22. Boyd, John W., and Phelps, E. Ray: A Comparison of the Experimental
    and Theoretical Loading Over Triangular Wings at Supersonic Speeds.
    NACA RM A50J17, 1951.

23. Hatch, John E., Jr., and Gallagher, James J.: Aerodynamic Character-
    istics of a 68.4° Delta Wing at Mach Numbers of 1.6 and 1.9 Over
    a Wide Reynolds Number Range. NACA RM L53I08, 1953.

24. Love, Eugene S., and Grigsby, Carl E.: A New Shadowgraph Technique
    for the Observation of Conical Flow Phenomena in Supersonic Flow
    and Preliminary Results Obtained for a Triangular Wing. NACA
    TN 2950, 1953.

25. Burcher, Marie A.: Compressible Flow Tables for Air. NACA TN 1952,
    1948.

TABLE I.- WING DIMENSIONS

Wing designation	Semiapex angle, deg	Sketch	Root chord, in.	Span, in.	Area, sq in.	Location of maximum thickness	$\frac{t}{c}$	Aspect ratio
1	30		3.897	4.500	8.77	0.18c	0.080	2.310
2	22		6.000	4.848	14.545	.18c	.080	1.616
3	17.91		5.990	3.876	11.59	:18c	.080	1.293
4	9.93		5.990	2.100	6.29	.18c	.080	.700
5	5		8.800	1.540	6.78	.18c	.080	.350
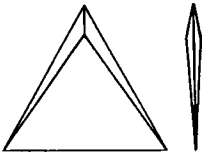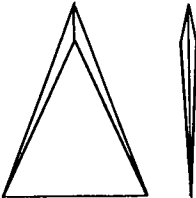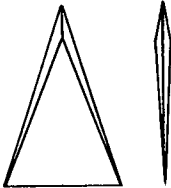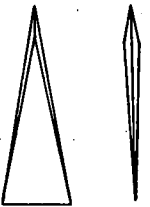
TABLE II.- THE COEFFICIENTS OBTAINED FROM SHOCK-EXPANSION

THEORY FOR A DOUBLE-WEDGE-SECTION AIRFOIL 8 PERCENT

THICK AT THE 18-PERCENT-CHORD POINT

$[M = 6.90]$

α, deg	c_N	c_C	c_L	c_D	L/D	C.P.
0	0	0.0122	0	0.0122	0	-----
1	.0128	.0122	.0126	.0124	1.02	0.328
2	.0256	.0123	.0252	.0132	1.91	.331
2.79	.0362	.0124	.0356	.0142	2.51	.331
5	.0671	.0129	.0657	.0187	3.51	.337
7.5	.1038	.0137	.1011	.0271	3.73	.345
10	.1443	.0148	.1395	.0397	3.51	.356
12.53	.1907	.0161	.1827	.0571	3.20	.367
15	.2426	.0175	.2298	.0797	2.88	.379
20	.3673	.0205	.3381	.1449	2.33	.400
25	.526	.0235	.4668	.2436	1.92	.418
27	.602	.0247	.525	.2953	1.78	.424
30	.732	.0279	.620	.3902	1.59	.430
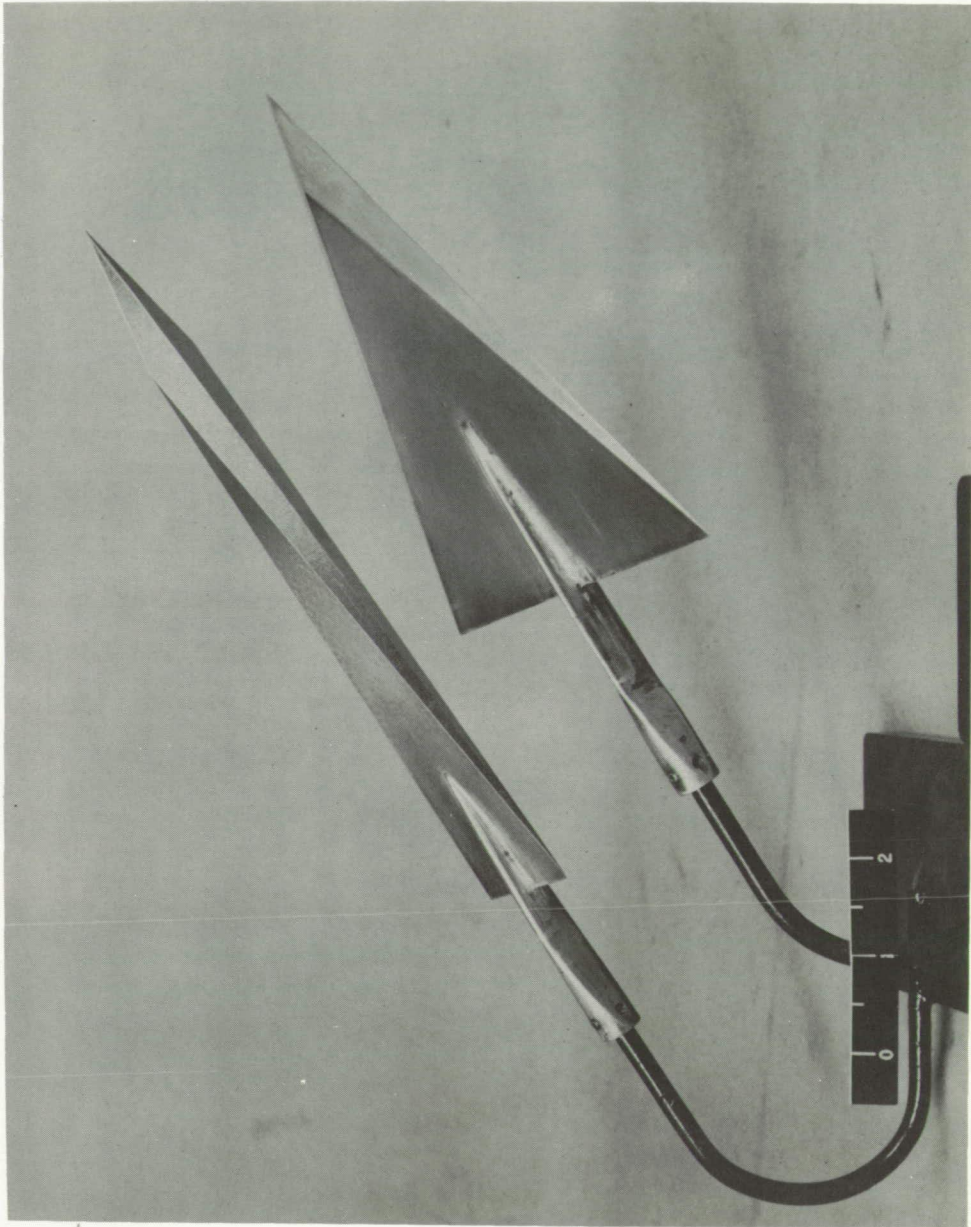
L-83508

(a) Wings 2 and 5.

Figure 1.- The wings with their mounting stings.

Wing	C_r	$\triangle C$	y	d
1	3.897	1.81	2.38	.16
2	6.000	2.00	2.38	.16
3	5.990	1.98	2.38	.16
4	5.990	1.98	2.38	.16
5	8.800	1.56	1.88	.13
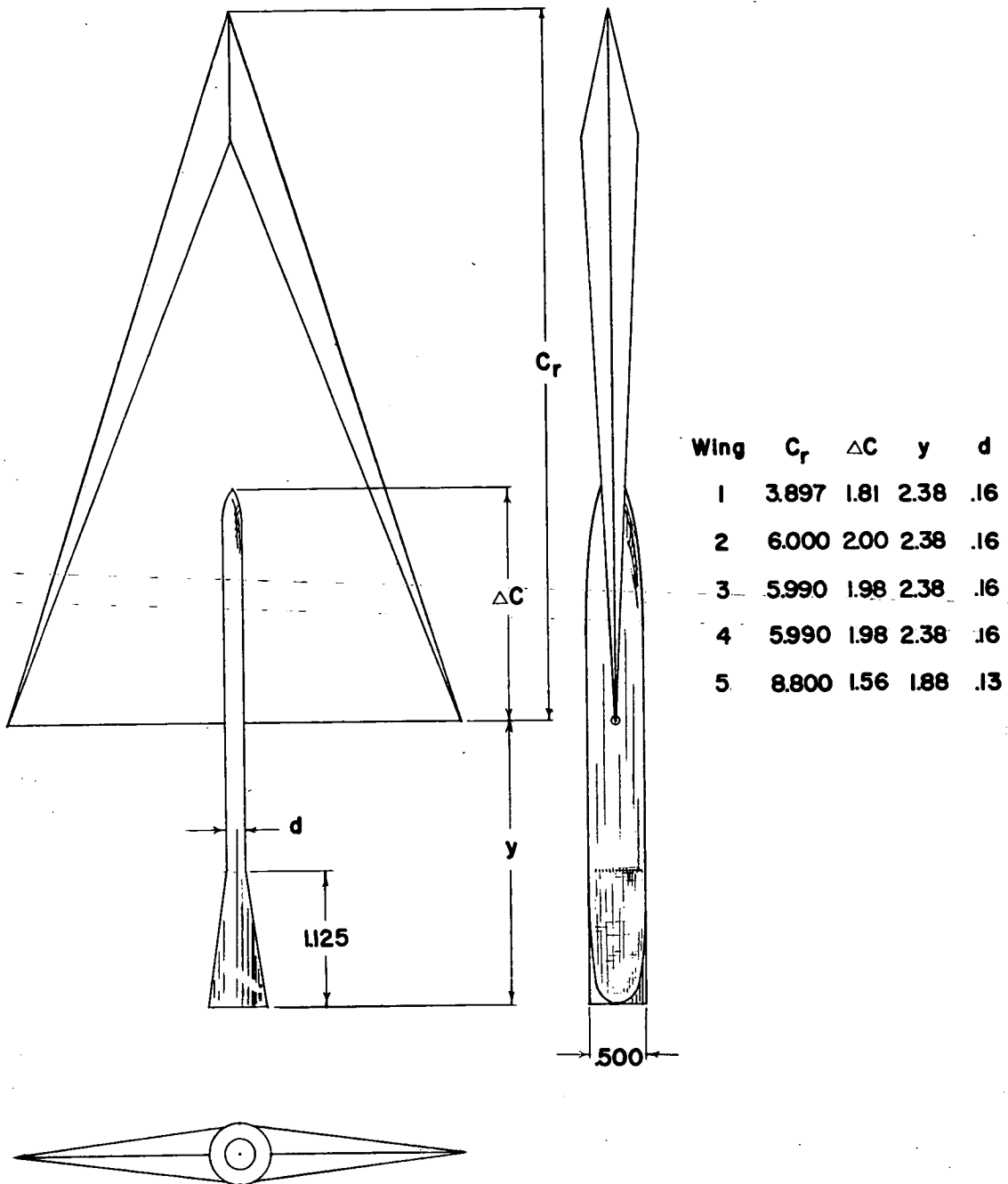
(b) Mounting sting with dimensions.   All dimensions are in inches.

Figure 1.- Concluded.
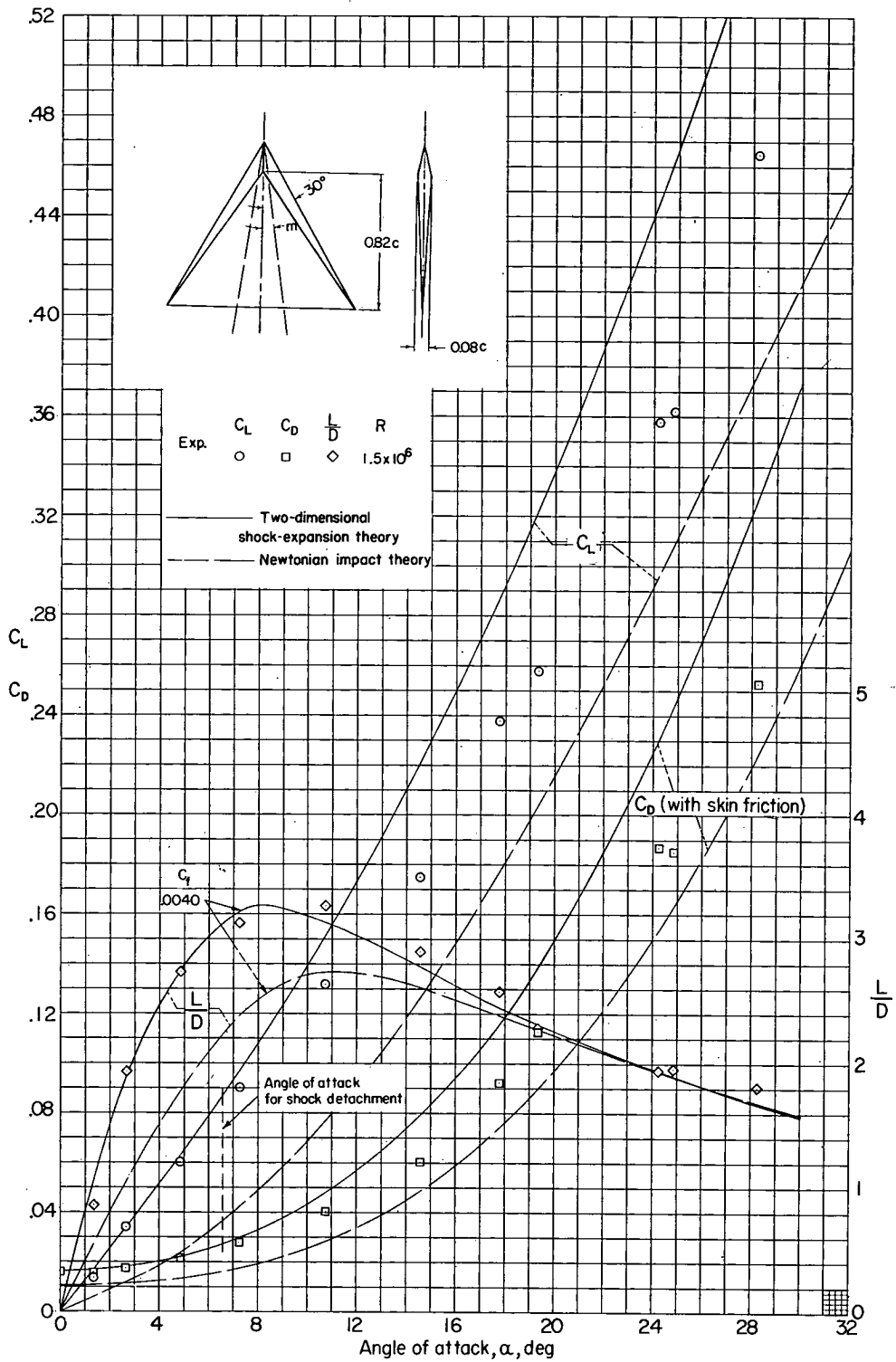
(a) $\epsilon = 30°$.

Figure 2.- The variation of the lift and drag coefficients with angle of
attack for the various delta wings tested. M = 6.9.

(b) $\epsilon = 22^{o}$.
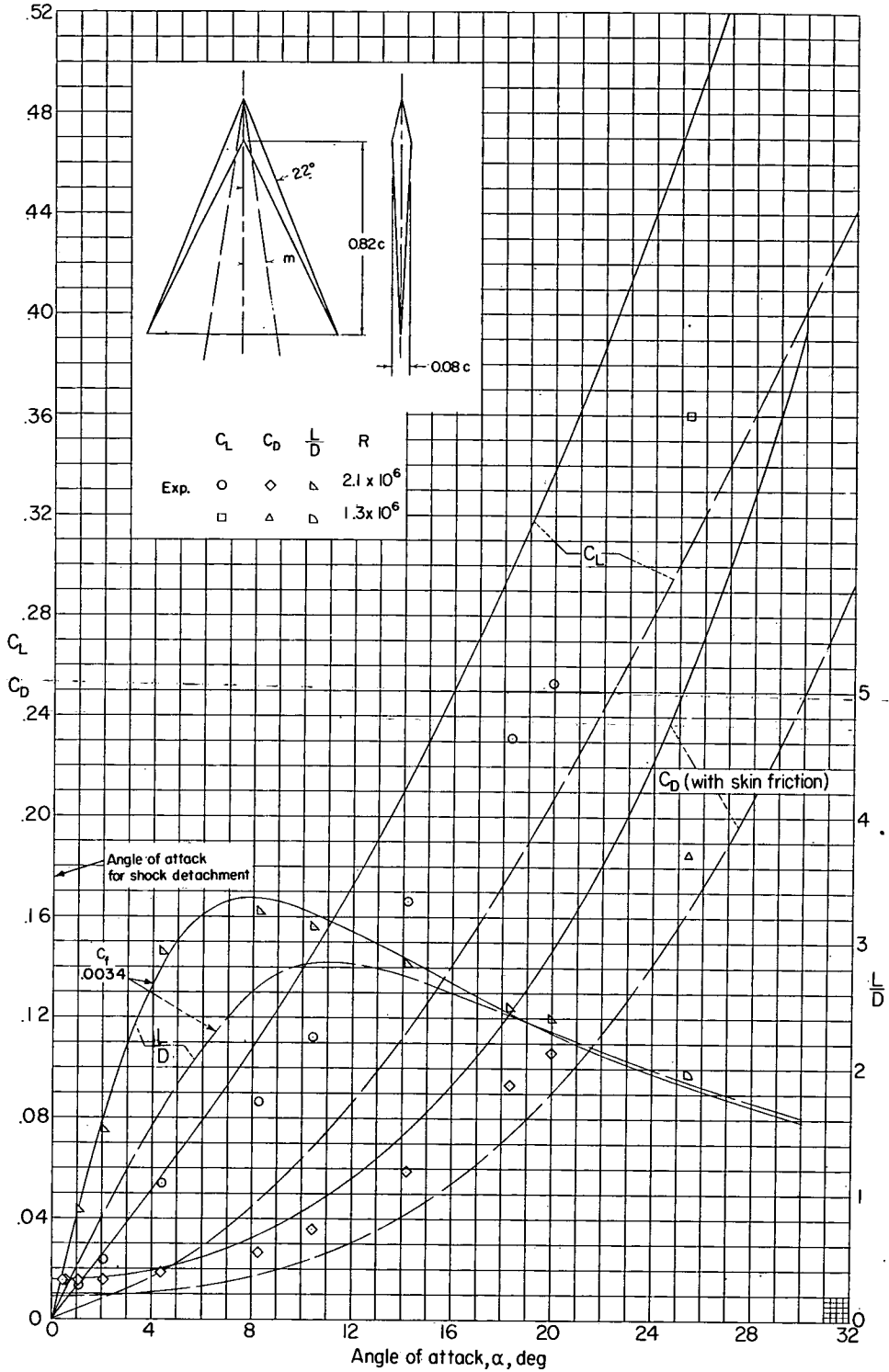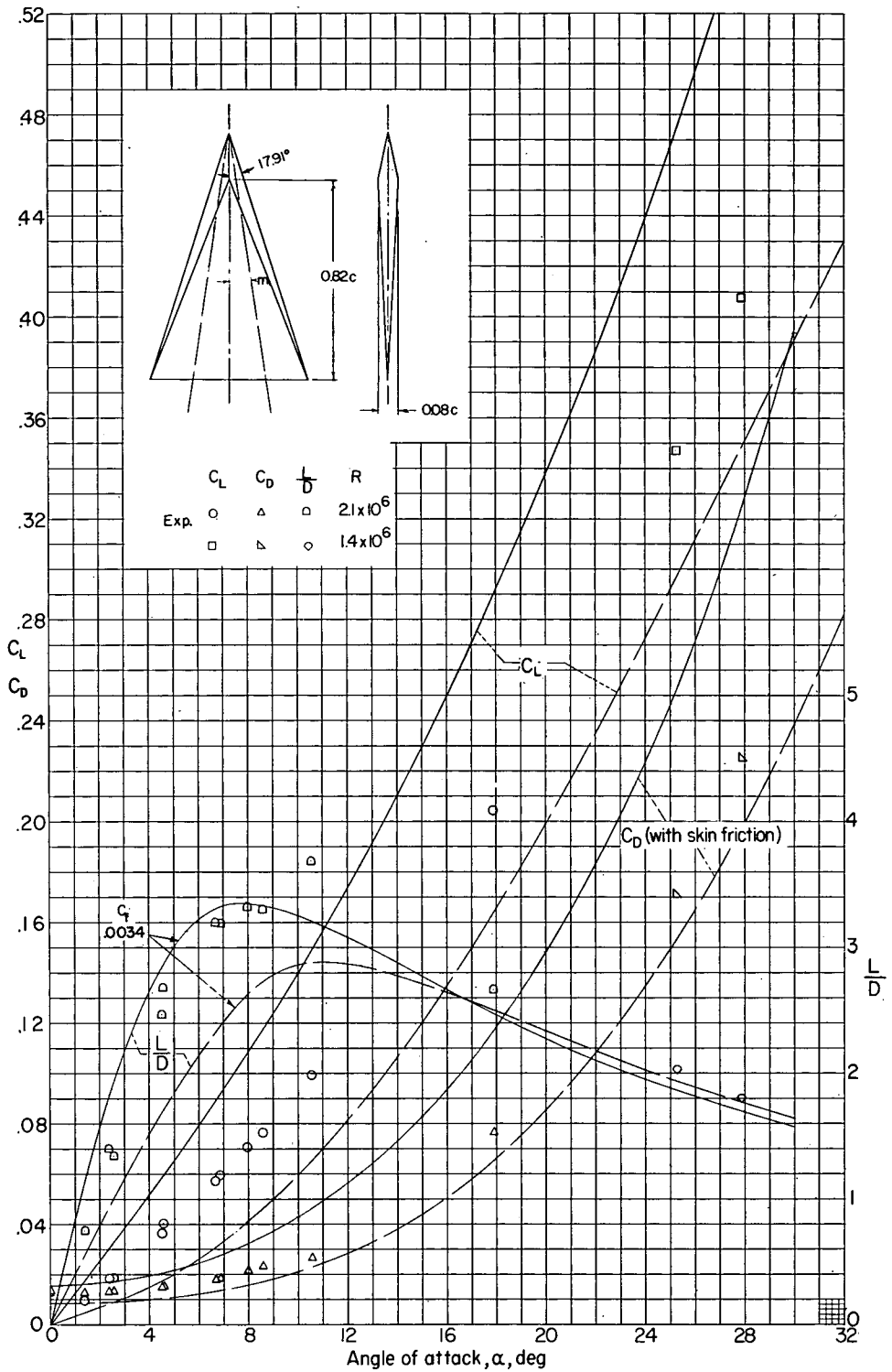
Figure 2.- Continued.

(c) $\epsilon = 17.91^{\circ}$.

Figure 2.- Continued.
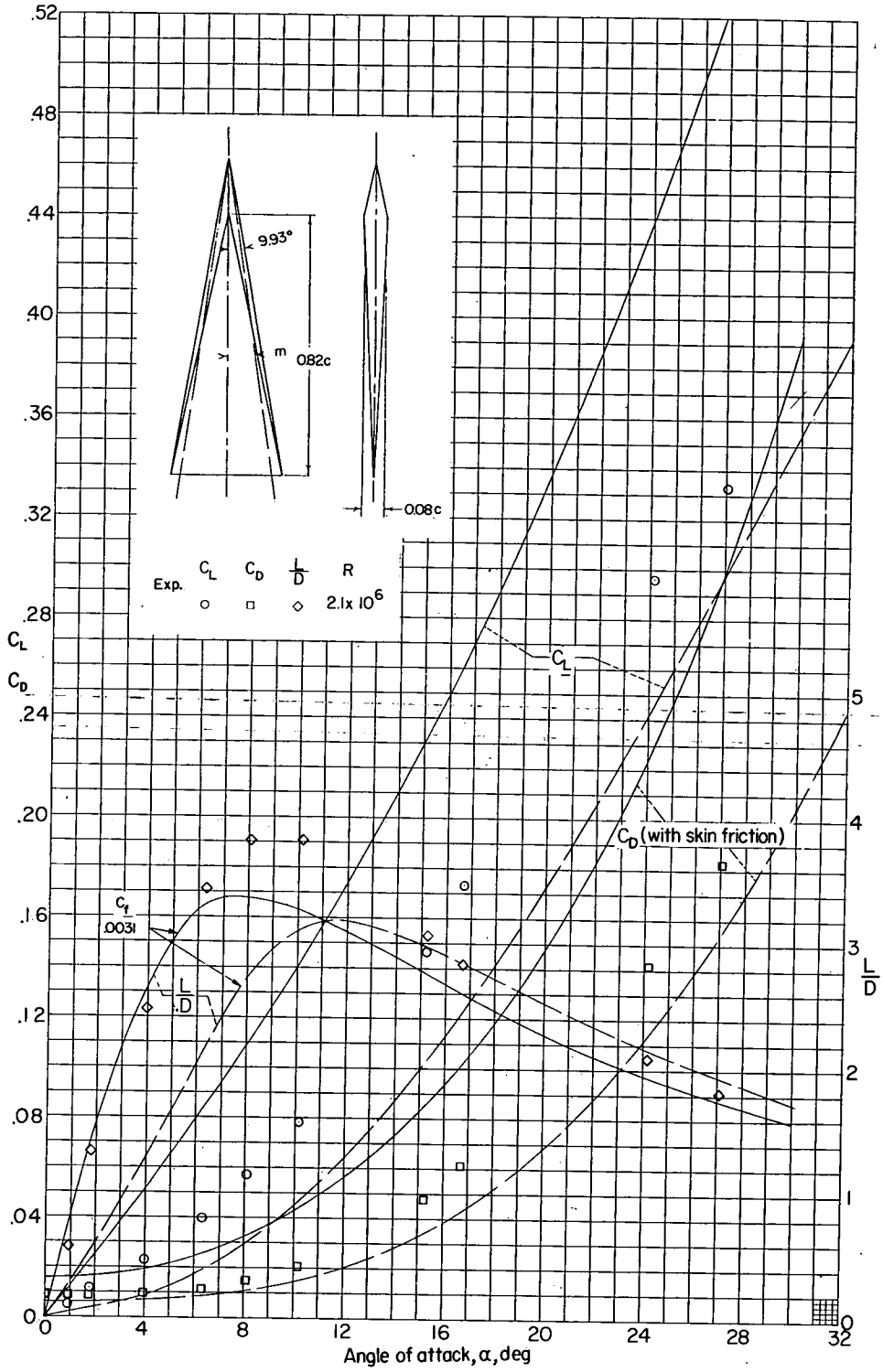
(d) $\epsilon = 9.93^\circ$.

Figure 2.- Continued.
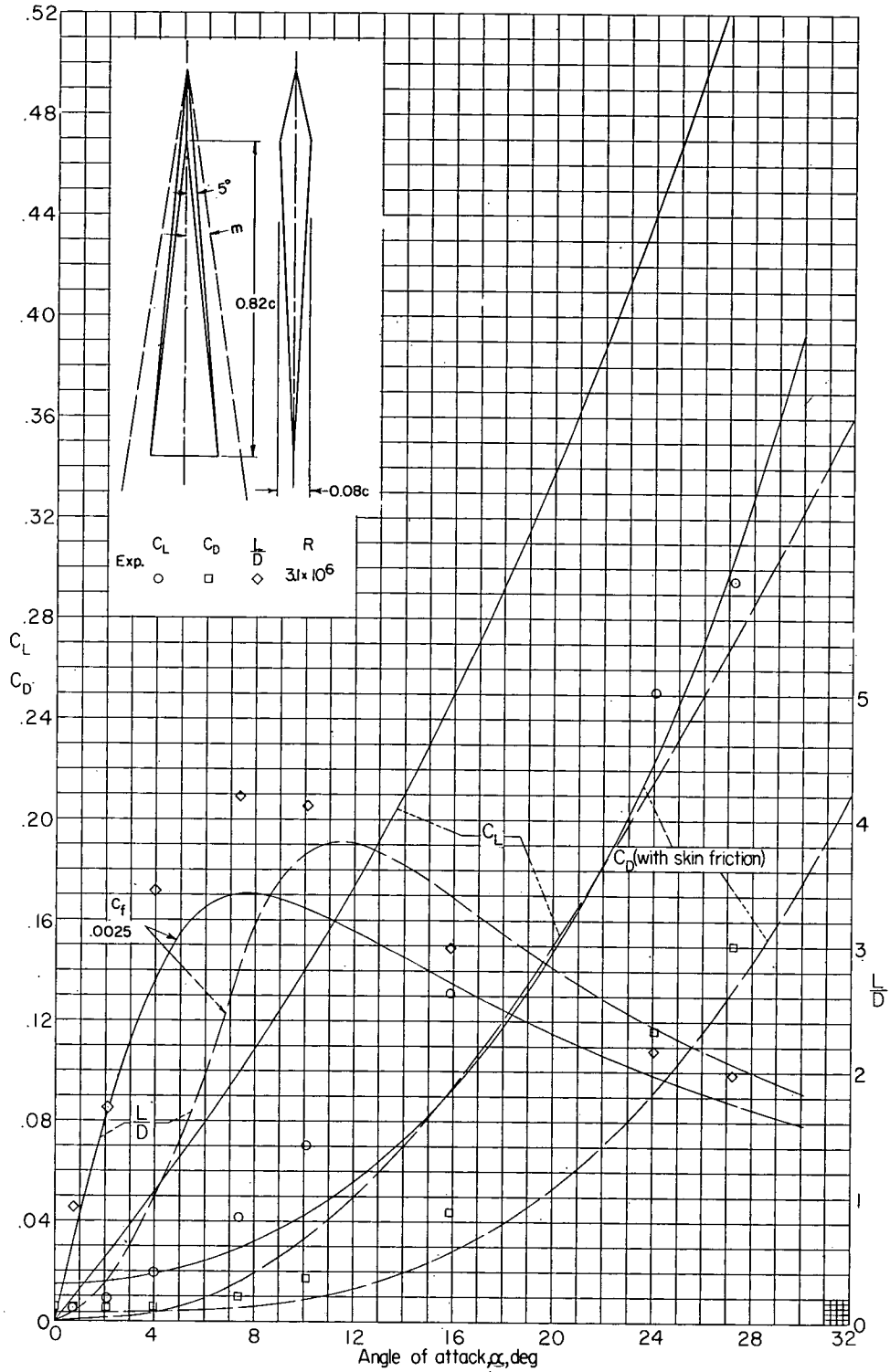
(e) $\epsilon = 5^{\circ}$.

Figure 2.- Concluded.
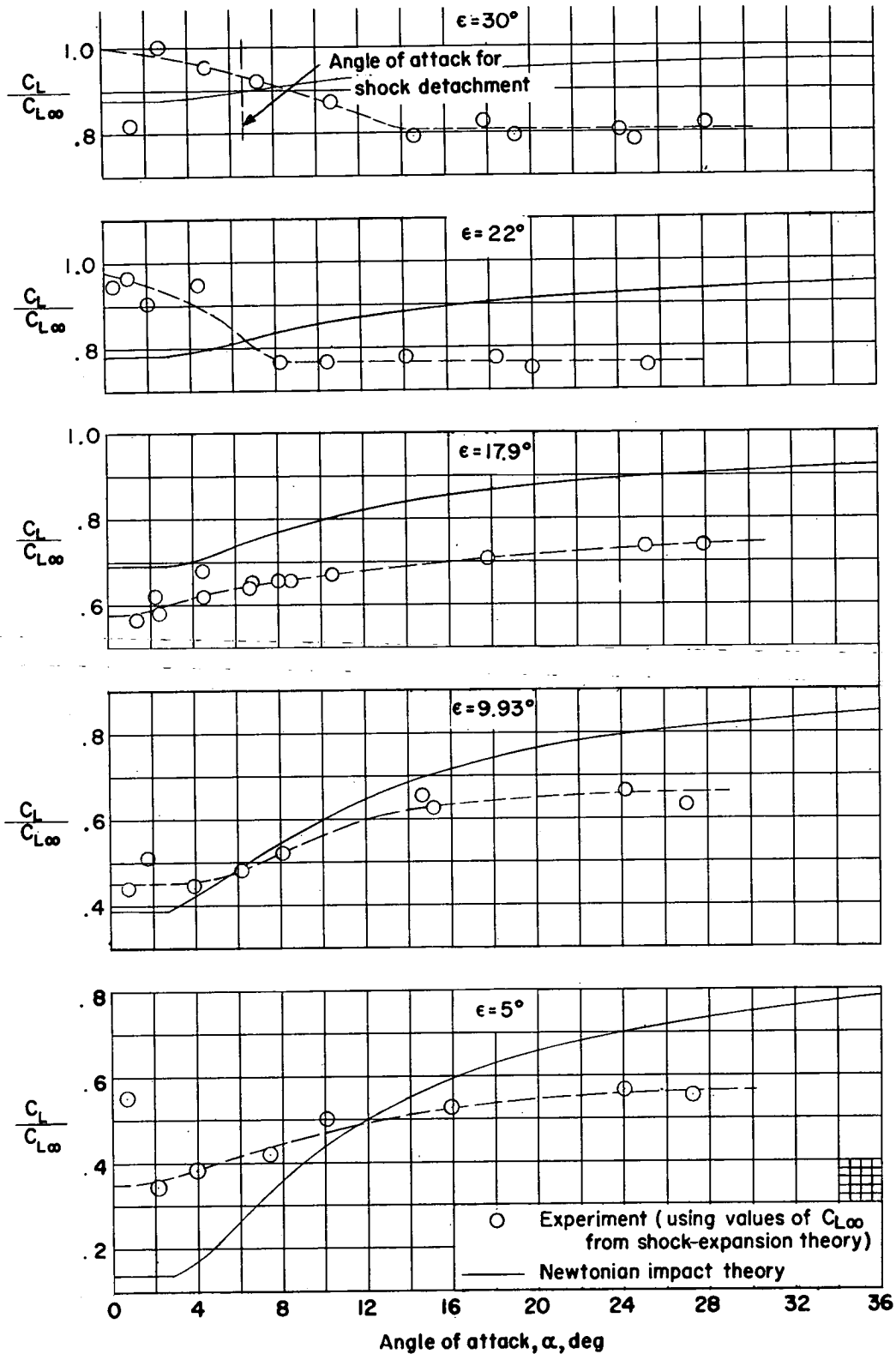
Figure 3.- The ratio of the lift coefficient of the delta wings to the two-dimensional lift coefficient as a function of angle of attack. M = 6.9.
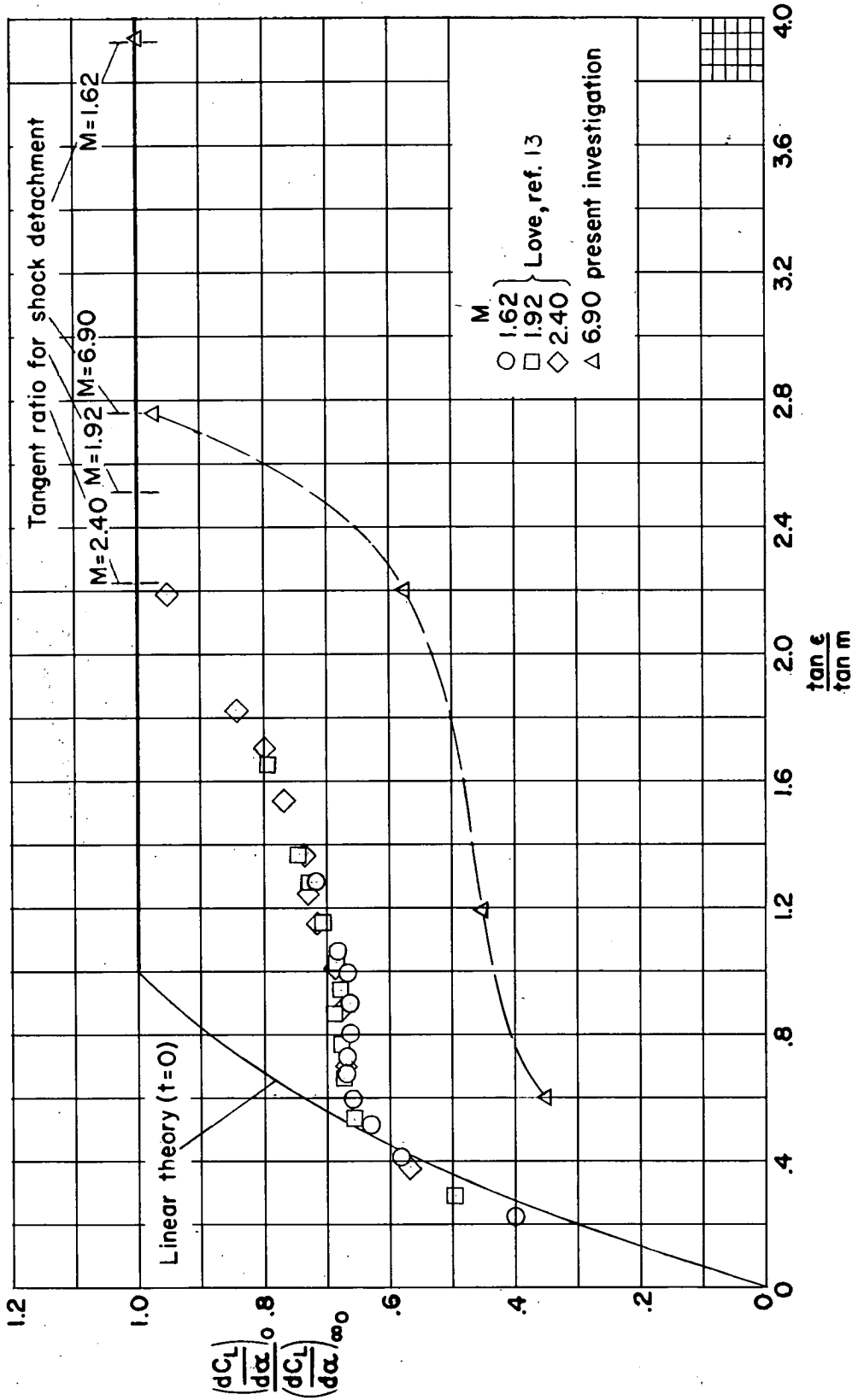
Figure 4.- The ratio of the lift-curve slope at zero angle of attack to the theoretical two-dimensional lift-curve slope at zero angle of attack as a function of the tangent ratio for various Mach numbers.
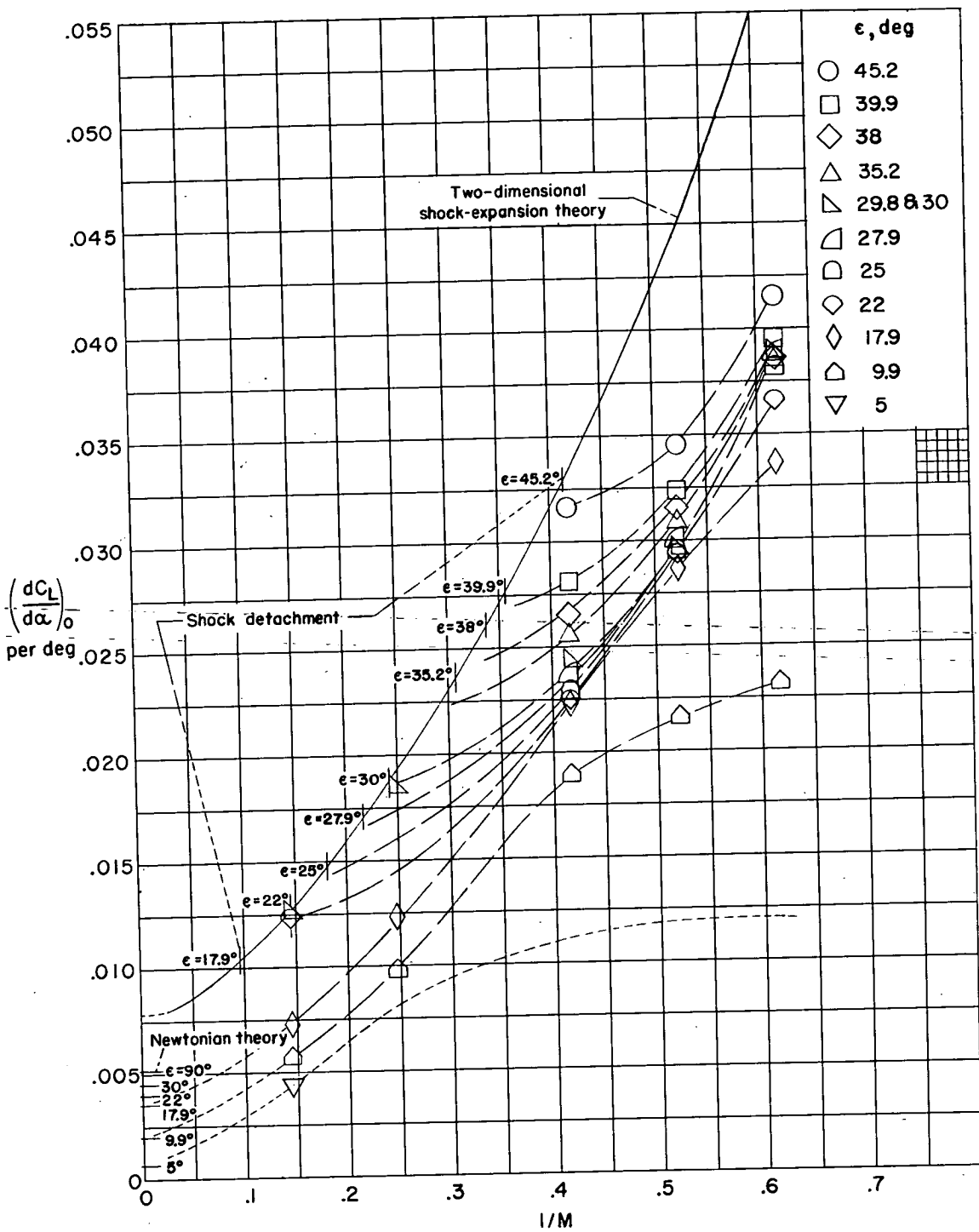
Figure 5.- The lift-curve slope of delta wings at zero angle of attack as a function of the reciprocal of the Mach number for various semiapex angles.
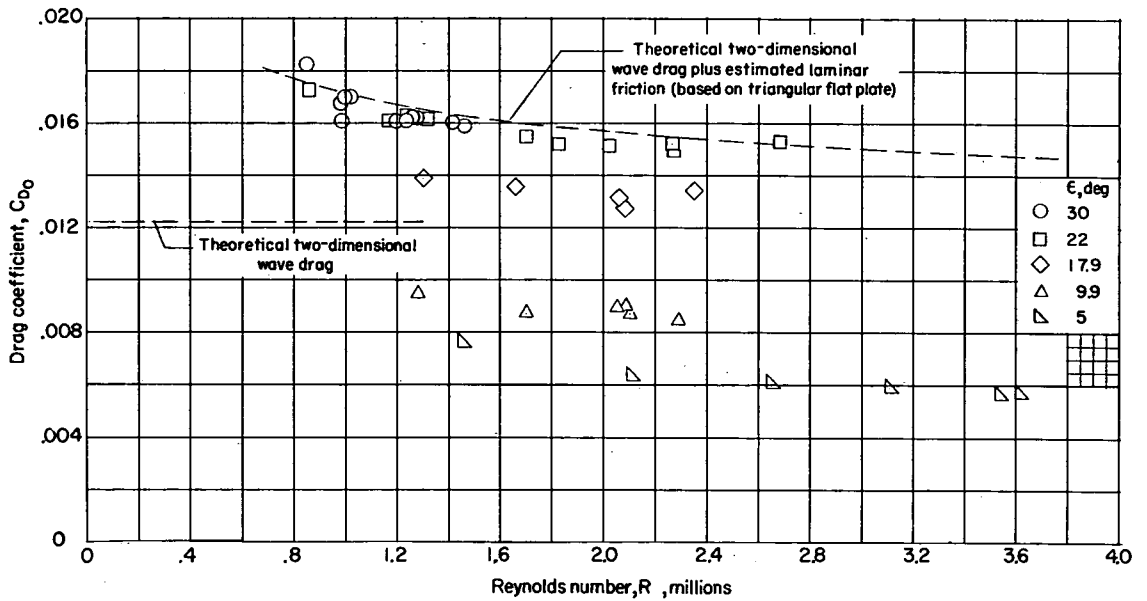
Figure 6.- The drag coefficient at zero angle of attack as a function of
the Reynolds number for various semiapex angles.   M = 6.9.
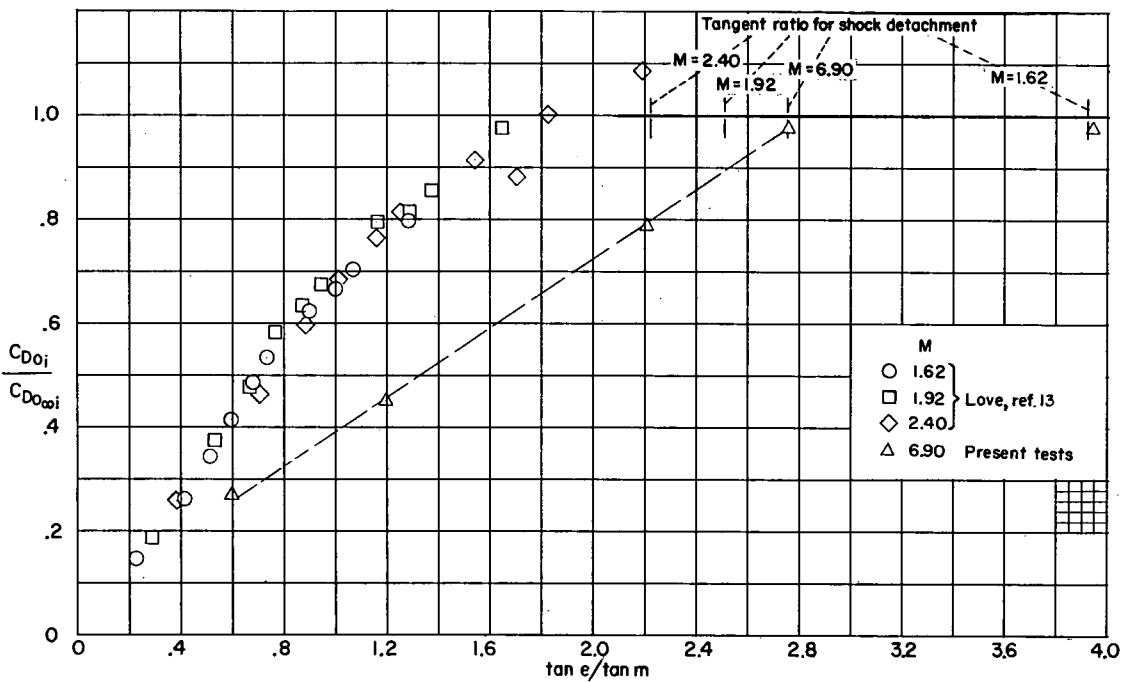
Figure 7.- The ratio of the drag at zero angle of attack to the two-
dimensional shock-expansion drag at zero angle of attack as a function
of the tangent ratio for various Mach numbers.
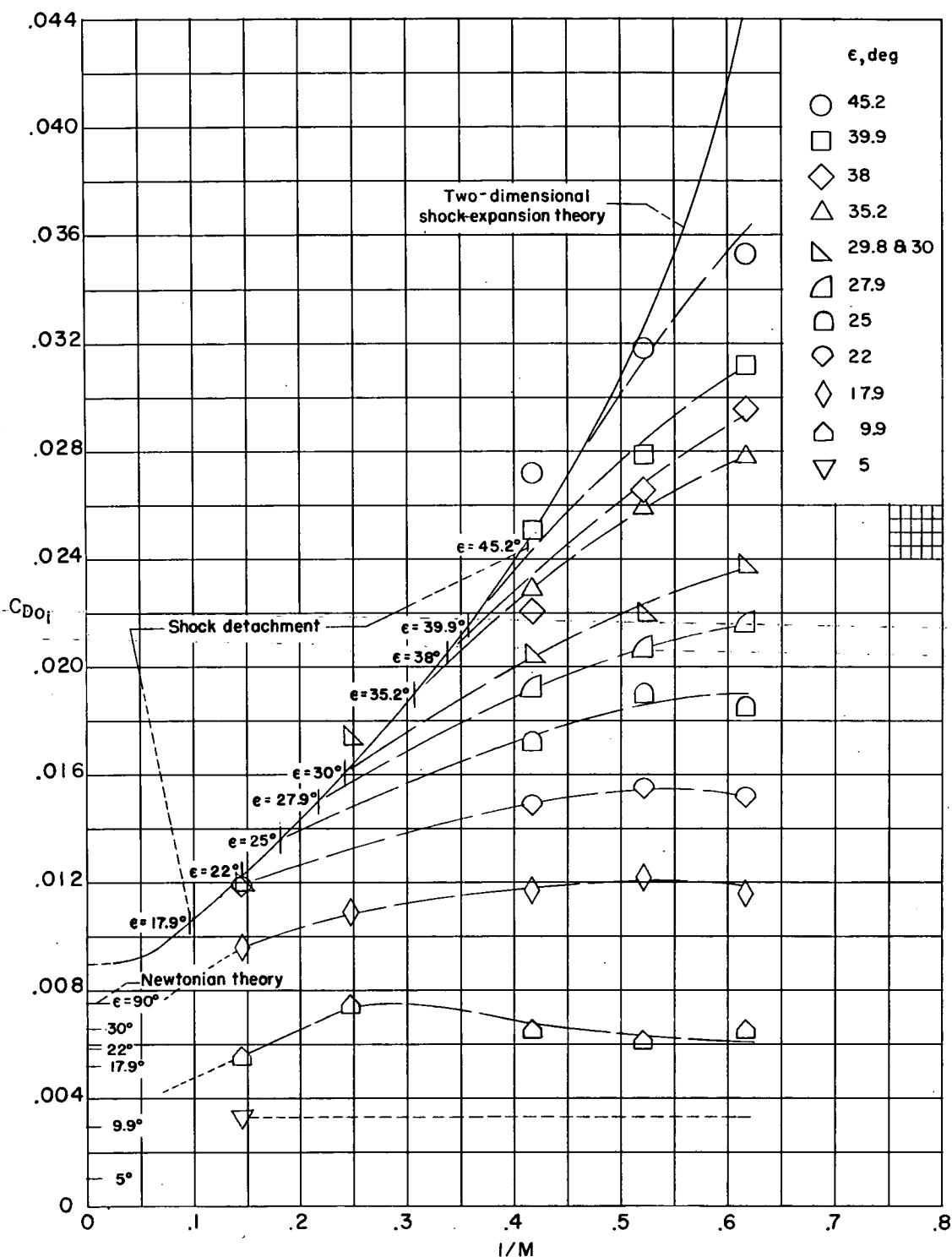
Figure 8.- The drag coefficient of delta wings at zero angle of attack as a function of the reciprocal of the Mach number for various semiapex angles.
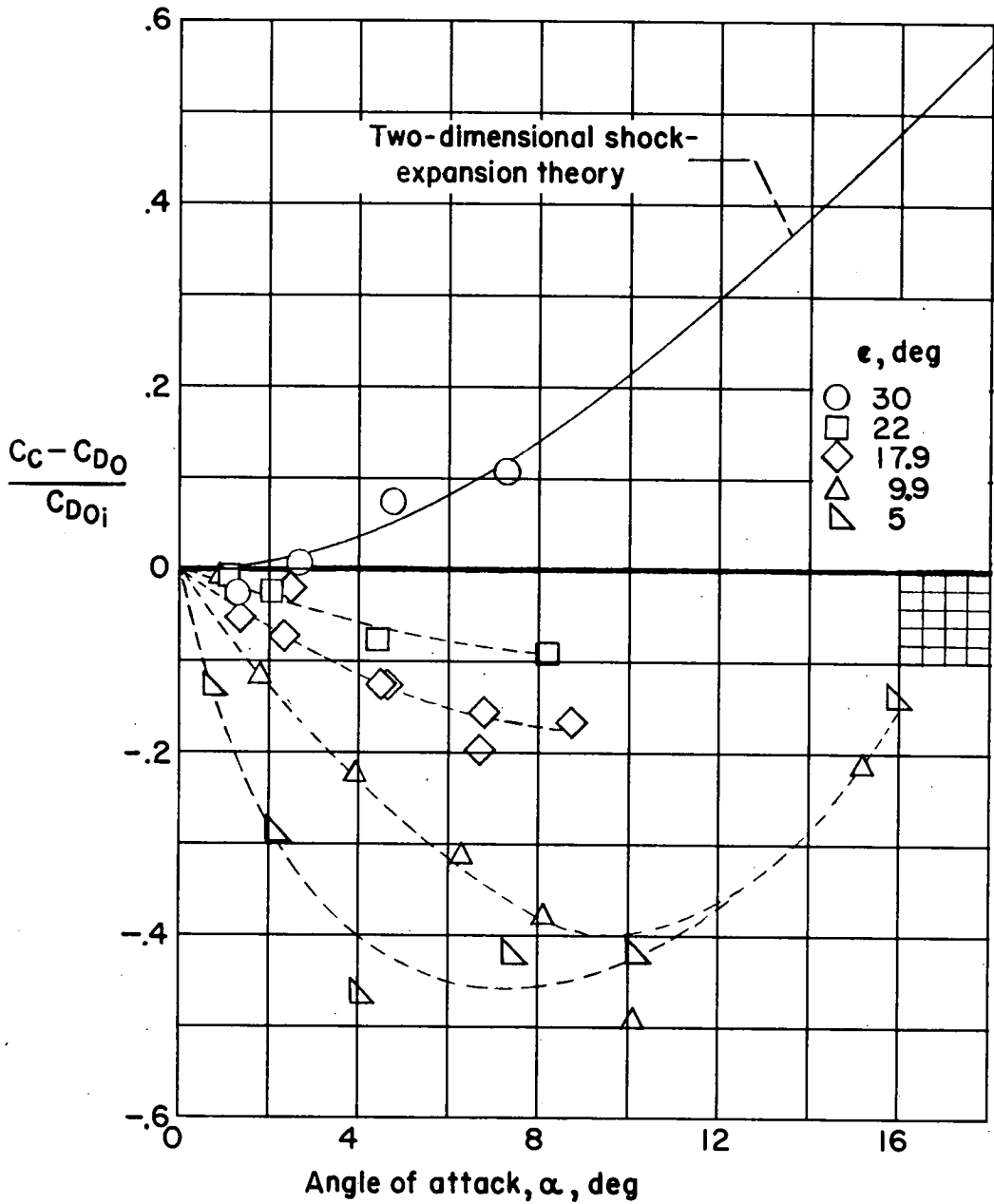
Figure 9.- The ratio of the change in chord-force coefficient from that at zero angle of attack to the estimated inviscid drag coefficient at zero angle of attack as a function of angle of attack.   M = 6.9.
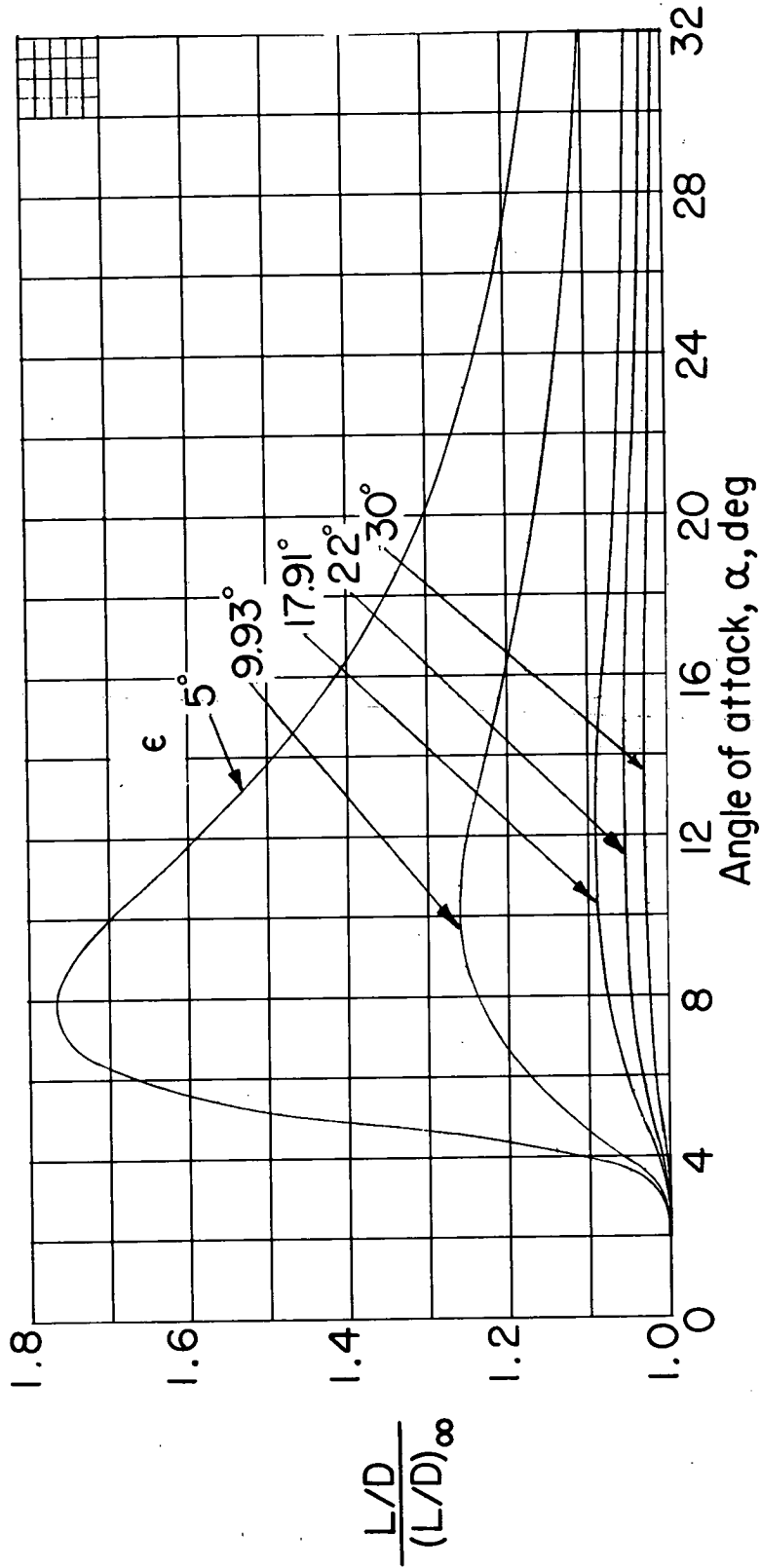
Figure 10.— Predictions of Newtonian theory for the lift-drag ratio as a
function of angle of attack for various semiapex angles.
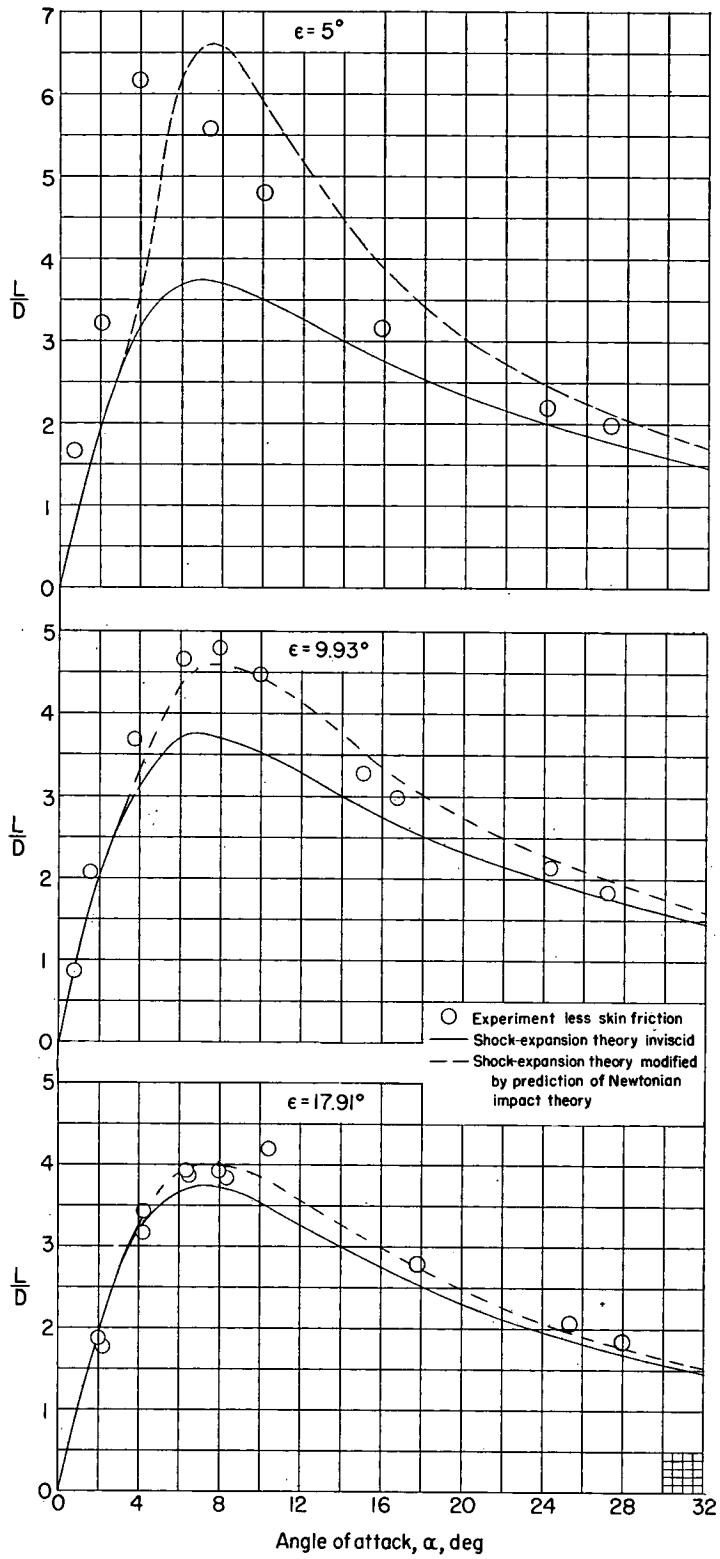
Figure 11.- Lift-drag ratio from experiment and theory as a function of
angle of attack.   M = 6.9.
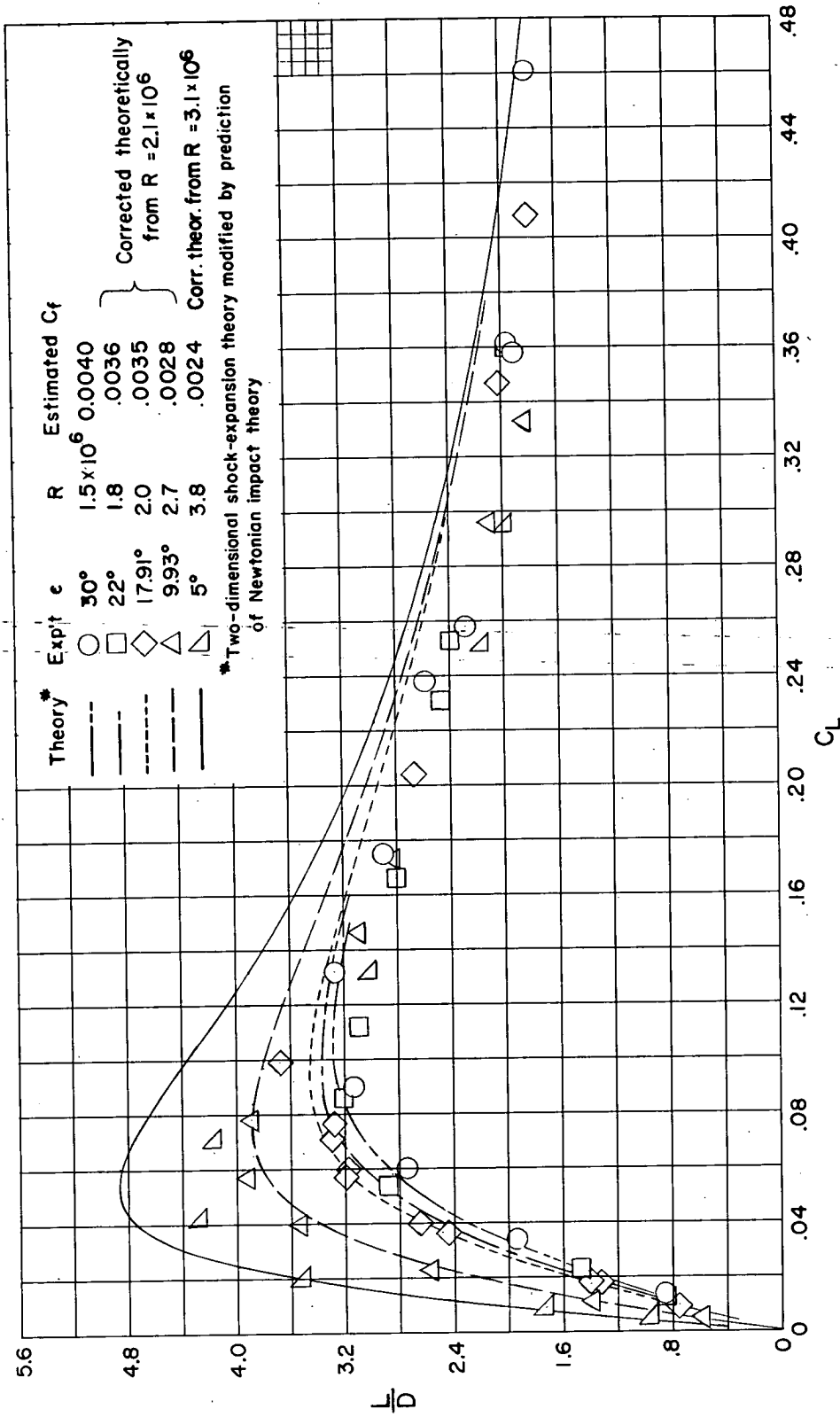
Figure 12.- The lift-drag ratio as a function of lift coefficient for
various semiapex angles where the plan-form area is maintained con-
stant. M = 6.9.
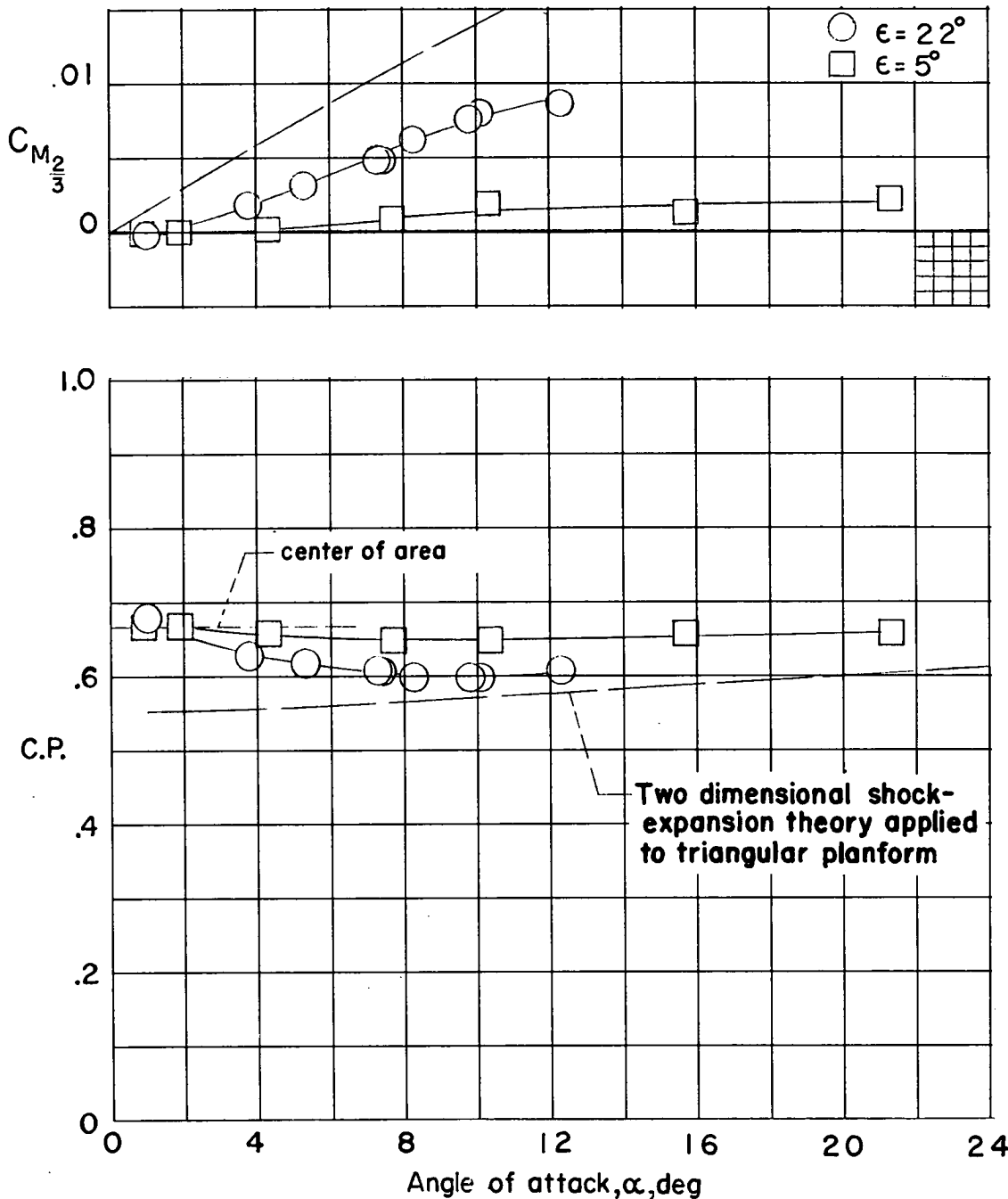
Figure 13.- The moment coefficient about the two-thirds chord point and center of pressure as a function of angle of attack. M = 6.9.
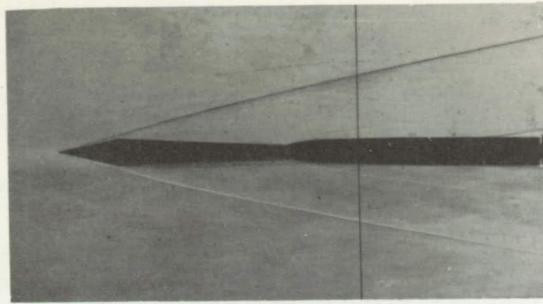
(a) $\alpha = 1.1°$.
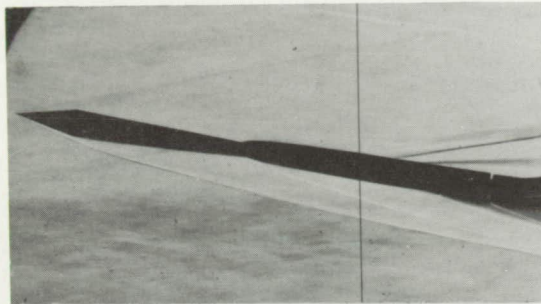
(b) $\alpha = 10.4°$.
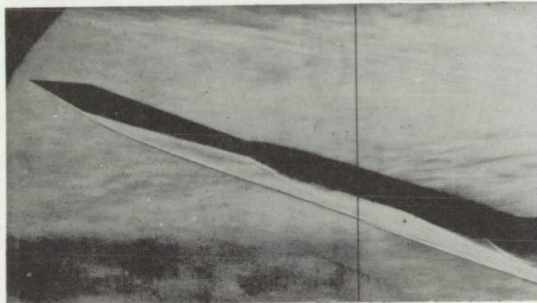
(c) $\alpha = 18.3°$.
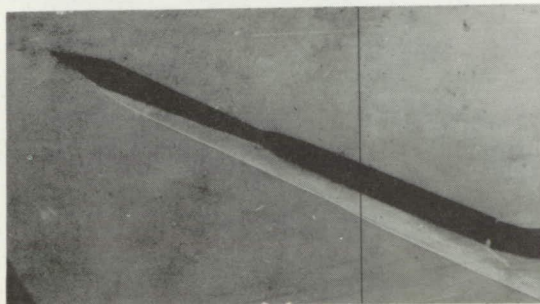
(d) $\alpha = 25.4°$.

L-85580

Figure 14.- Side-view schlieren photographs of wing 2 ($\epsilon = 22°$) at vari-
ous angles of attack. M = 6.9.

(a) $\alpha = 0.3^{\circ}$.

(b) $\alpha = 8^{\circ}$.
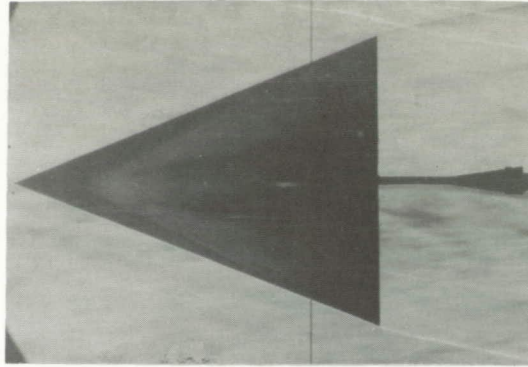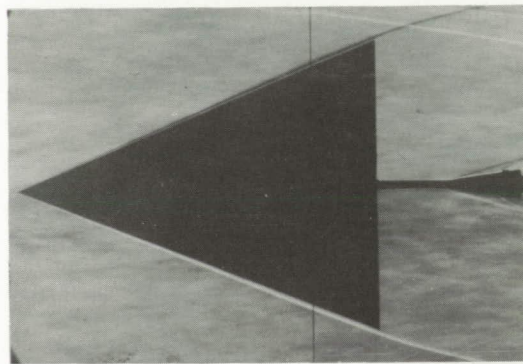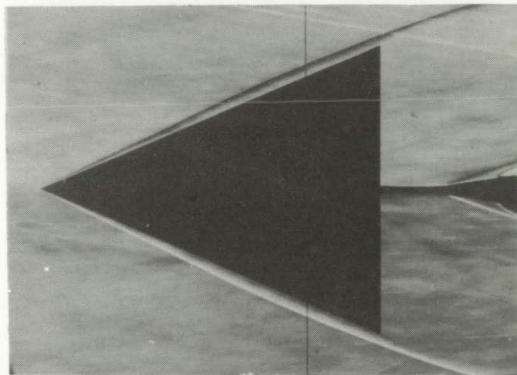
L-85581

(c) $\alpha = 18.8^{\circ}$.

Figure 15.- Top-view schlieren photographs of wing 2 ($\epsilon = 22^{\circ}$) at various angles of attack. M = 6.9.
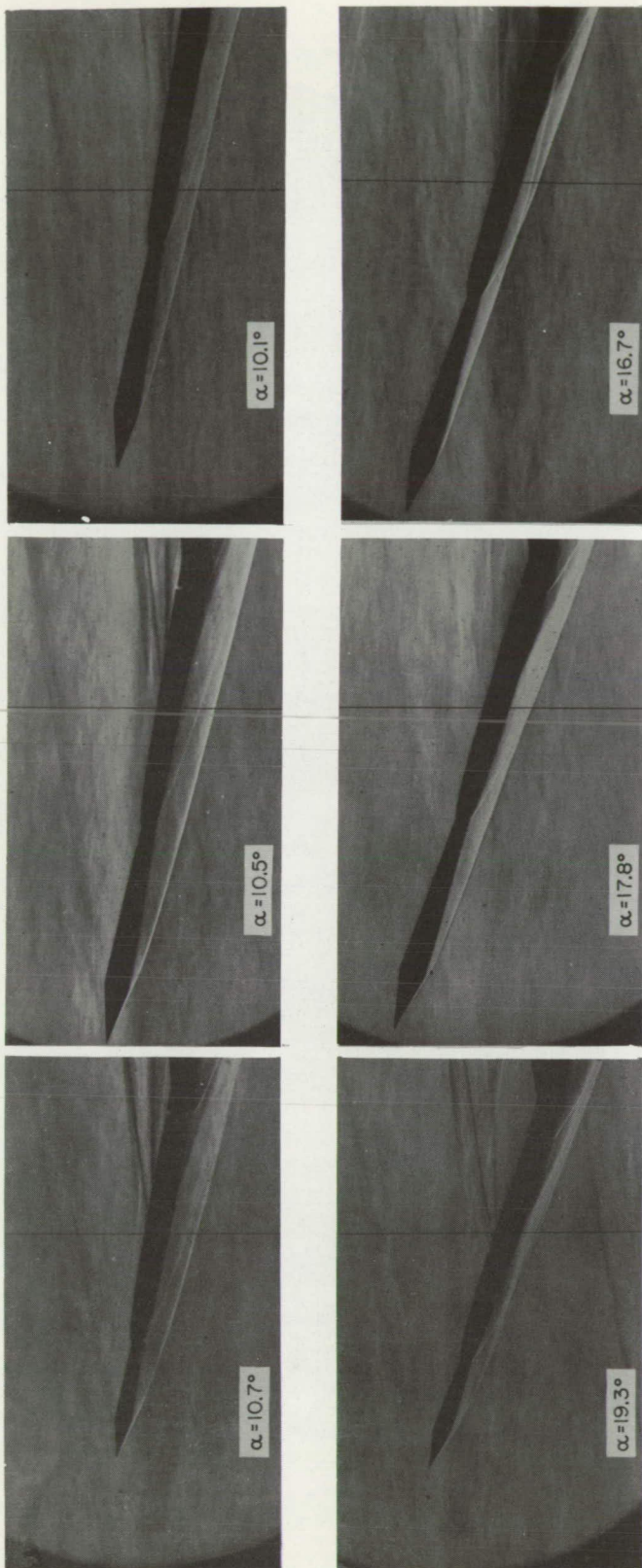
(a) $\epsilon = 30^\circ$.   (b) $\epsilon = 17.9^\circ$.   (c) $\epsilon = 9.9^\circ$.   L-85582

Figure 16.- Side-view schlieren photographs of wings 1, 3, and 4 at two angles of attack.   M = 6.9.

(a)   α = 0.5°.

(b)   α = 0.1°.

(c)   α = 10.1°.

(d)   α = 15.9°.
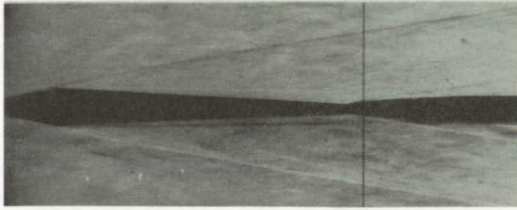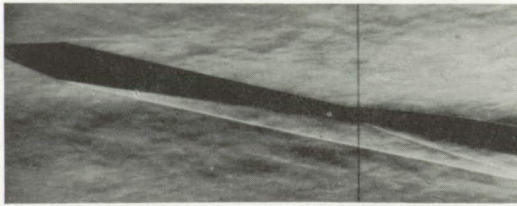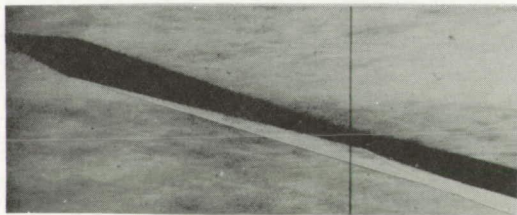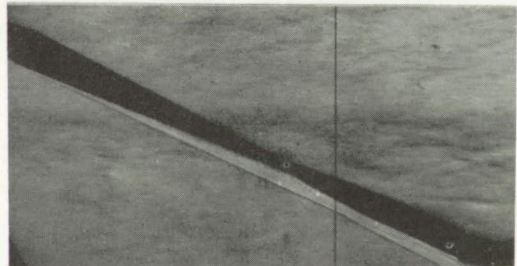
(e)   α = 24°.   L-85583

Figure 17.- Top- and side-view schlieren photographs of wing 5 (ε = 5°)
                at various angles of attack.   M = 6.9.
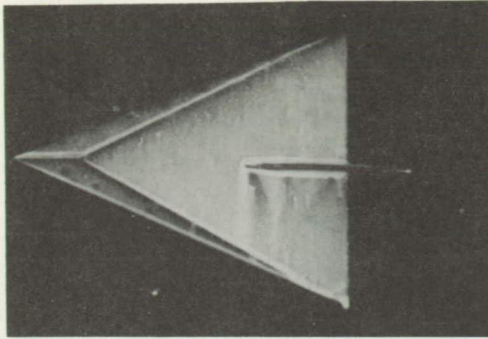
(a) α = 0.3°; no flow.   (b) α = 0.3°; upper surface.
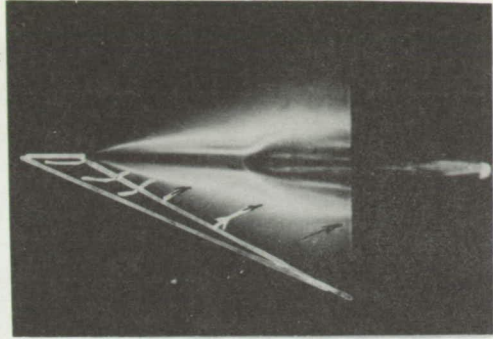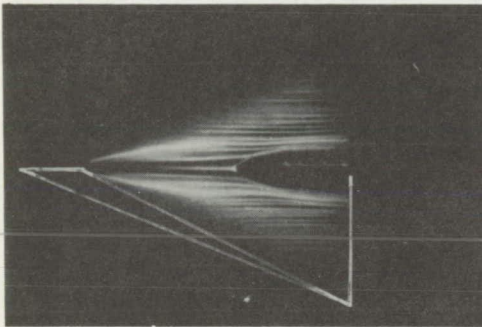
(c) α = 6.9°; lower surface.   (d) α = 8°; upper surface.
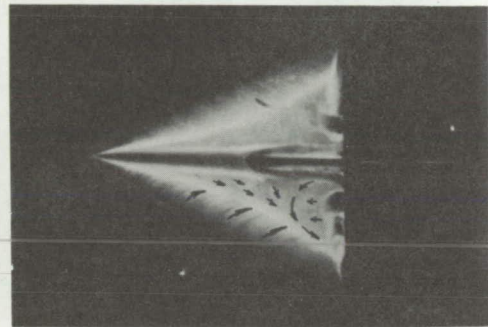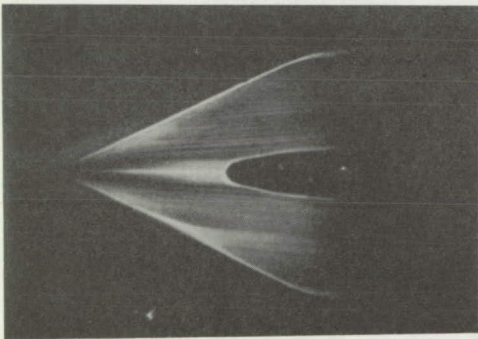
L-85584
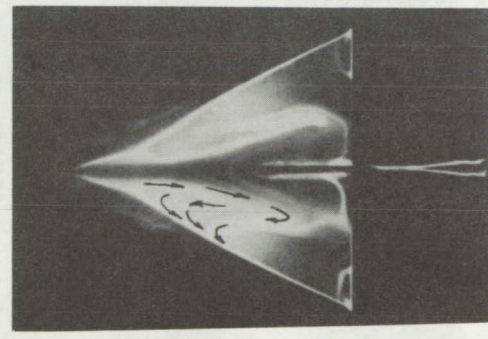
(e) α = 18.8°; lower surface.   (f) α = 19.2°; upper surface.

Figure 18.- Surface fluid flow studies of wing 2 (ε = 22°) at various
angles of attack. M = 6.9; R = 2.3 × 10^6.
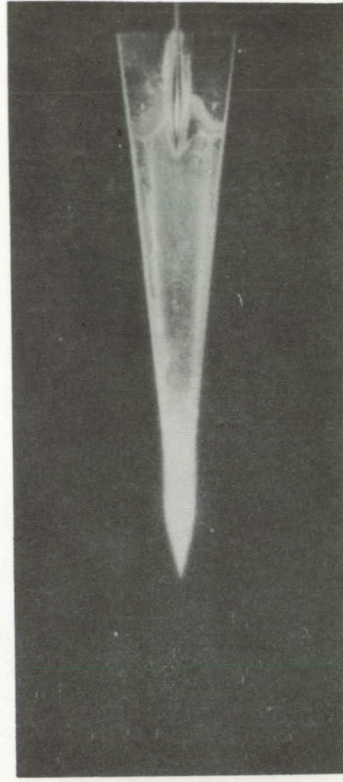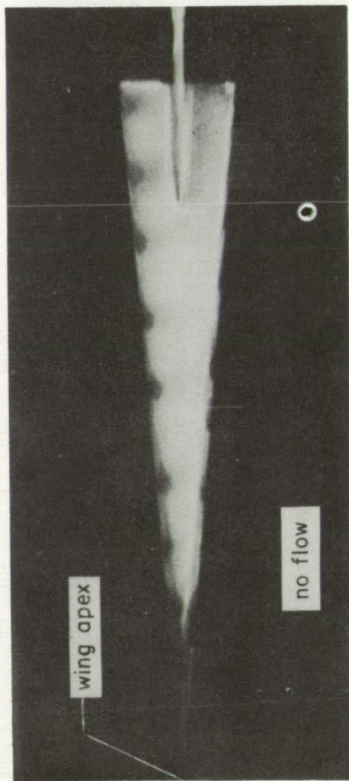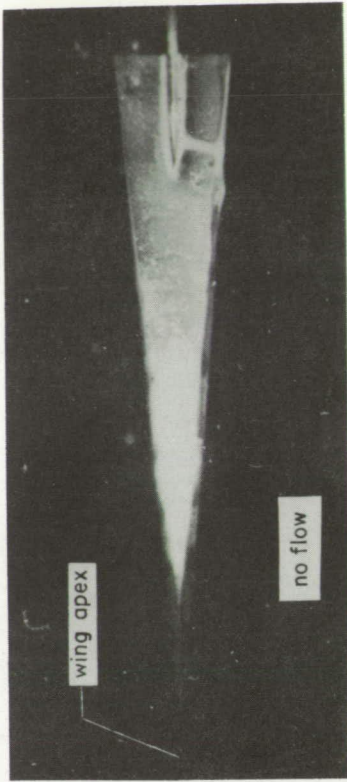
(a) $\alpha = 7.6°$.

(b) $\alpha = 18.5°$. L-85585

Figure 19.- Surface fluid flow studies on the upper surface of wing 5 ($\epsilon = 5°$) at two angles of attack. M = 6.9; R = 3.3×10^6.